ORIGINAL ARTICLE

MicrobiologyOpen

WILEY

DNA stable-isotope probing reveals potential key players for microbial decomposition and degradation of diatom-derived marine particulate matter

Ying Liu[1] 🟢 | Jiasong Fang[2,3,4] | Zhongjun Jia[5] | Songze Chen[1] | Li Zhang[6] | Wei Gao[5]

[1]State Key Laboratory of Marine Geology, Tongji University, Shanghai, China

[2]Shanghai Engineering Research Center of Hadal Science and Technology, Shanghai Ocean University, Shanghai, China

[3]Laboratory for Marine Biology and Biotechnology, Qingdao National Laboratory for Marine Science and Technology, Qingdao, China

[4]Department of Natural Sciences, Hawaii Pacific University, Honolulu, HI, USA

[5]State Key Laboratory of Soil and Sustainable Agriculture, Institute of Soil Science, Chinese Academy of Sciences, Nanjing, China

[6]State Key Laboratory of Geological Process and Mineral Resources, Faculty of Earth Sciences, China University of Geosciences, Wuhan, China

Correspondence
Jiasong Fang, Shanghai Engineering Research Center of Hadal Science and Technology, Shanghai Ocean University, Shanghai, China.
Email: jsfang@shou.edu.cn

Li Zhang, State Key Laboratory of Geological Process and Mineral Resources, Faculty of Earth Sciences, China University of Geosciences, Wuhan, Hubei, China.
Email: lizhang@cug.edu.cn

Abstract

Microbially mediated decomposition of particulate organic carbon (POC) is a central component of the oceanic carbon cycle, controlling the flux of organic carbon from the surface ocean to the deep ocean. Yet, the specific microbial taxa responsible for POC decomposition and degradation in the deep ocean are still unknown. To target the active microbial lineages involved in these processes, ^{13}C-labeled particulate organic matter (POM) was used as a substrate to incubate particle-attached (PAM) and free-living microbial (FLM) assemblages from the epi- and bathypelagic zones of the New Britain Trench (NBT). By combining DNA stable-isotope probing and Illumina Miseq high-throughput sequencing of bacterial 16S rRNA gene, we identified 14 active bacterial taxonomic groups that implicated in the decomposition of ^{13}C-labeled POM at low and high pressures under the temperature of 15°C. Our results show that both PAM and FLM were able to decompose POC and assimilate the released DOC. However, similar bacterial taxa in both the PAM and FLM assemblages were involved in POC decomposition and DOC degradation, suggesting the decoupling between microbial lifestyles and ecological functions. Microbial decomposition of POC and degradation of DOC were accomplished primarily by particle-attached bacteria at atmospheric pressure and by free-living bacteria at high pressures. Overall, the POC degradation rates were higher at atmospheric pressure (0.1 MPa) than at high pressures (20 and 40 MPa) under 15°C. Our results provide direct evidence linking the specific particle-attached and free-living bacterial lineages to decomposition and degradation of diatomic detritus at low and high pressures and identified the potential mediators of POC fluxes in the epi- and bathypelagic zones.

KEYWORDS
decomposition, free-living microorganisms, New Britain Trench, particle-attached microorganisms, particulate organic carbon

1 | INTRODUCTION

Organic matter produced by phytoplankton in the surface ocean is exported to the deep ocean and the seabed via, mostly, sinking particulate organic matter (POM) by the processes of the biological pump (Azam & Malfatti, 2007; Eppley & Peterson, 1979; Falkowski, 1998; Volk & Hoffert, 1985). It is estimated that sinking particulate organic carbon (POC) (10^2–10^4 μm diameter; Verdugo et al., 2004) is transported to the deep ocean with a global rate of 2–13 Pg C year^{-1} (Boyd & Trull, 2007; Eppley & Peterson, 1979; Lima, Lam, & Doney, 2014). During descent, the sinking POC flux attenuates sharply with depth as a result of decomposition of POC and release of dissolved organic carbon (DOC) from abiotic (disaggregation and fragmentation) and biotic processes (zooplankton consumption and microbial remineralization) (Burd & Jackson, 2009; DeLong, Franks, & Alldredge, 1993; Simon, Grossart, Schweitzer, & Ploug, 2002; Steinberg et al., 2008; Turner, 2015; Wilson, Steinberg, & Buesseler, 2008). Approximately 90% of the sinking POC is remineralized in the upper 1,000 m, and only 0.1%–0.3% of the POC can reach the seafloor and is ultimately buried in sediments (Arístegui, Agustí, Middelburg, & Duarte, 2005; Arístegui, Gasol, Duarte, & Herndld, 2009; Hedges, 1992; Wakeham & Lee, 1993).

Marine microorganisms play a critical role in the decomposition and remineralization of POC (Anderson & Ryabchenko, 2009; Anderson & Tang, 2010; Azam & Malfatti, 2007; Fang et al., 2015). It has been hypothesized that the particulates act as carbon- and nutrient-rich hotspots, and the particle-attached microorganisms (PAM) secrete exoenzymes to decompose the particles and release dissolved organic carbon (Simon et al., 2002). PAM solubilize POM faster than they are able to take up the released DOC, leading to the formation of carbon- and nutrient-rich DOC plumes, streaming behind the POC particulates. The released DOC supports PAM and the free-living microorganisms (FLM) in the surrounding water for their growth and respiration (Azam & Long, 2001; Fang et al., 2015; Kiørboe & Jackson, 2001; Li et al., 2015). Thus, microbial decomposition and transformation of POM controls organic carbon (OC) fluxes delivered from the surface ocean to the deep ocean, and heterotrophic microorganisms play an essential role in the process (e.g., Belcher et al., 2016; Karl, Knauer, & Martin, 1988; Steinberg et al., 2008). Understanding POC decomposition and degradation processes is critical to assess the sequestration and storage of carbon in the ocean and oceanic carbon cycling.

Hydrostatic pressure is a critical parameter in affecting microbial physiology (Bubendorfer et al., 2012; Marietou & Bartlett, 2014), abundance (Grossart and Gust, 2009; Marietou & Bartlett, 2014), metabolic activity (Tamburini, Garcin, Ragot, & Bianchi, 2002; Tamburini et al., 2006; Tamburini et al., 2003; Turley, 1993), diversity, and community structure (Grossart and Gust, 2009; Marietou & Bartlett, 2014; Tamburini et al., 2006, 2009). Piezophiles refer to pressure-loving microorganisms, which grow preferentially at high pressure than atmospheric pressure. Piezotolerant bacteria had optimal growth at atmospheric pressure (Fang et al., 2010). For instance, deep-sea bacterium *Photobacterium profundum* SS9

increased the proportion of unsaturated fatty acids at high pressure (Allen et al., 1999), *Shewanella putrefaciens* CN-32 possesses dual flagellar system (Bubendorfer et al., 2012) under high pressure conditions. High pressure reduced bacterial cell numbers (Grossart and Gust, 2009; Marietou & Bartlett, 2014), decreased microbial metabolic activity (Tamburini et al., 2006; Tamburini et al., 2002; Tamburini et al., 2003; Turley, 1993) and organic matter degradation rates (Tamburini, Boutrif, Garel, Colwell, & Deming, 2013). High pressure increased the relative abundance of Gammaproteobacteria and *Cytophaga-Flavobacter* cluster when prokaryotes incubated with diatom detritus (Tamburini et al., 2006) or fecal pellets (Tamburini et al., 2009). Laboratory experiments showed that high pressure caused an increase in the relative proportion of Alphaproteobacteria in a coastal environment (Marietou & Bartlett, 2014).

Despite its importance, it remains a principal challenge to identify and quantify the relative importance of various microbes involved in these processes. There has been no direct evidence linking specific bacterial lineages to POM decomposition and DOM degradation. Some studies indicate that bacterial activity on sinking particles in the deep ocean is inadequate to account for the attenuating POC flux with depth (Karl et al., 1988). Others suggest that the free-living bacteria, rather than particle-attached bacteria, are the primary mediators of particulate decomposition in the ocean's interior (Cho & Azam, 1988; Karl et al., 1988). Furthermore, there have been contrasting estimates on the contributions of PAM in particle decomposition and remineralization. Smith, Simon, Alldredge, and Azam (1992) estimated that 97% of the hydrolysates produced by bacteria in marine snow were released, with 3% being utilized by PAM in the aggregates (Smith et al., 1992). In another study, Belcher et al. (2016) showed that PAM respiration represents a minor portion (3%–16%) of POC attenuation in the upper water column, but becomes more important (10%–65%) in the deep, suggesting great variations in rates of the processes with depth (Belcher et al., 2016). Knowing which types of microorganisms break down POM and degrade DOM may be useful in the assessment of factors that control OC flux from the surface ocean to the deep ocean. As the succession of microbial communities often occurs with depth in the ocean, studying the response of microbial communities to POM at different depths can provide clues about linkages between microbial niche specialization and their resource utilization (e.g., Lauro et al., 2009).

Stable-isotope probing (SIP) is a powerful technique that directly links specific functional microorganisms to a particular biogeochemical process (Radajewski, Ineson, Parekh, & Murrell, 2000). This method is based on the premise that metabolically active microbes that assimilate stable-isotope-labeled substrates would incorporate the rare isotope (e.g., ^{13}C) into cellular macromolecules (e.g., DNA, phospholipid fatty acids, etc.), that can be detected by molecular microbiological techniques, thereby enabling the identification and quantification of the functionally active microorganisms (Radajewski et al., 2000). In the present study, we used DNA stable-isotope probing to target the active microbial taxa involved in decomposition and degradation of POM and DOM by incubating microorganisms enriched from shallow (75 m) and deep waters (2,000 and 4,000 m) of

the New Britain Trench with ^{13}C-labeled POM. We hypothesize that PAM and FLM perform different functions in the ocean, that is, POC decomposition by the former and DOC degradation by the latter. We further postulate that the divided functions between PAM and FLM become undivided with increasing pressure in the deep ocean, that is, both groups of microbes can perform the same functions, POC decomposition and DOC degradation. The objective of this study was to gain insight into the microbial-mediated decomposition and degradation processes of diatom-derived marine particulate organic carbon (POC), by mimicking POC sinking from the surface ocean to the deep ocean (increase in hydrostatic pressure) and examining the changes in community structure of particle-attached and free-living microorganisms, the processes they participated in (decomposition and degradation), and the rates of carbon utilization by these microbes.

2 | MATERIALS AND METHODS

2.1 | Sampling

Seawater samples were collected from the E station (06°02.1243′S, 151°58.5042′E) (Figure A1) of the New Britain Trench (NBT) during the cruise of M/V _Zhangjian_ in September 2016. Samples were taken at three depths, 75-, 2000-, and 4000-m, by using a SBE-911Plus CTD with Niskin bottles (Sea-Bird Inc.). The seawater samples were not kept under in situ pressure prior SIP incubations. The physical and chemical parameters of the seawater samples in the water column of NBT can be seen in Table A1.

    About 1 L seawater sample from each depth was filtered sequentially through a 47-mm 3 μm pore size polycarbonate (PC) membrane (Merck Millipore Ltd.) to collect the particle-attached microbes, and a 47-mm 0.22 μm pore size PC membrane to collect the free-living bacterial assemblages (Eloe et al., 2011). A total of six filters were used for collecting PAM or FLM from seawater at each depth. Three filters were used for the total DNA extraction and community diversity analysis. The other three filters were used for subsequent SIP incubations (see below).

2.2 | Stable-isotope probing experiments

2.2.1 | Production of ^{13}C-labeled particulate organic matter (POM)

The planktonic diatom species _Thalassiosira weissflogii_ (strain CCMA-102), one of the most common diatom species in the global surface ocean, was selected for the ^{13}C-labeled tracer experiment. The diatoms were cultured either with added ^{13}C-labeled $NaHCO_3$ or nonlabeled $NaHCO_3$ (control), in the f/2 media prepared in a 5.5 L Erlenmeyer flask, with 5 L sterile artificial seawater (ASW). The ASW contained (w/v%) the following: 2.12 NaCl, 0.34 Na_2SO_4, 0.06 KCl, 0.008 KBr, 0.0058 H_3BO_3, 0.00028 NaF, 0.96 $MgCl_2 \cdot 6H_2O$, 0.13 $CaCl_2 \cdot 2H_2O$, 0.0022 $SrCl_2 \cdot 6H_2O$, 0.029 $NaH^{13}CO_3$ in distilled

water (Berges, Franklin, & Harrison, 2001), supplement with $NaSiO_3$ (Guillard, 1975), 250 ml _Thalassiosira weissflogii_ suspension (precultured for 20 days). The $NaH^{13}CO_3$ solution was prepared by dissolving 1.5 g $NaH^{13}CO_3$ in 50 ml sterile double-distilled H_2O (ddH_2O) and filtered through a 0.22 μm polycarbonate filter (Pasotti, Troch, Raes, & Vanreusel, 2012). After 30 days of growing in an illumination incubator at 20°C and a 12-hr, 12-hr light/dark regime, diatom detritus, ^{13}C-labeled and nonlabeled (control) were collected by centrifugation (Beckman Coulter) at 11,180 _g_ for 10 min. The collected diatom detritus was lyophilized in a Lyophilizer (Christ Corp.) at −44°C for 48 hr. The dry diatom detritus was ground with liquid nitrogen, and autoclaved at 121°C for 20 min, and then stored at −20°C until use. The percentage of the ^{13}C-labeled and ^{12}C-control for diatom detritus was determined to be 71.7% and 1.3%, respectively.

2.2.2 | High pressure incubation

Particle-attached microbial and FLM were obtained from serial filtrations as described above, the three filters for collecting PAM or FLM via filtration of seawater were added directly into the pouches for SIP incubations. The collected particle-attached and free-living microbes were incubated with the added bacteria-free detrital particulate organic matter in separate cultures, designated as 75 (2000/4000)-m-[13]C (^{12}C)-PAM (FLM), at in situ pressure (0.1, 20, and 40 megapascal, MPa) and 15°C under dark condition for 30 days, using air-tight pouches. The media contained 60 ml sterile artificial seawater, 0.2 g ^{13}C-labeled diatom detritus (≥0.7 μm pore size), and 20 ml Fluorinert™ (3M™ Corp.). Fluorinert was added to the pouches to serve as a source of oxygen to the cultures (Fang, Uhle, Billmark, Bartlett, & Kato, 2006; Kato, Sato, & Horikoshi, 1995). Prior to use, Fluorinert was saturated by bubbling high-purity oxygen for 8–10 hr at 4°C and then filtered through a 0.22 μm polycarbonate filter (Fang et al., 2006). The control was prepared using nonlabeled detritus as a growth substrate. All cultures were done in triplicate. Growth of PAM and FLM plateaued after 30 days.

    It must be emphasized that the in situ temperature was around 2°C at 2,000 and 4,000 m depths at our sampling sites (Table A1), much lower than the incubation temperature (15°C). For this test of concept study, we used 15°C, instead of the in situ temperature, in microbial cultivation, in order to generate enough biomass for subsequent molecular microbiological study.

2.3 | Determining the concentration and $\delta^{13}C$ of POC and DOC

An aliquot of 10 ml culture was filtered through 25-mm 0.7 μm pore size glass fiber filter (Whatman) which was precombusted in a muffle furnace at 450°C for 5 hr. The collected filter membrane and filtrate were used for POC and DOC concentration measurements, respectively. In preparation for POC and DOC analysis, the collected filters were pickled with 12 M HCl for 24 hr in fume cupboards

and then dried at 50°C for 24 hr in an oven, and the filtrate was acidized with 20 μl 12 M HCl. The concentration of POC and DOC was measured by a PE2400 Series II CHNS/O analyzer (Perkin Elmer) and a TOC-VCHP analyzer (Shimadzu Corp.), respectively, at the Institute of Soil Science, Chinese Academy of Sciences, Nanjing, China. The $\delta^{13}C$ of POC and DOC was determined by an Isotope Ratio Mass Spectrometer (Thermo Scientific) at the Third Institute of Oceanography, Xiamen, China.

## 2.4 | DNA extraction and SIP gradient fractionation

After 30 days incubation, an aliquot of 10 ml culture was centrifuged at 10,000 rpm for 5 min to collect cell biomass. The PC filters for PAM and FLM filtrations at day 0 were cut into pieces and then transferred to 2 ml sterilized centrifuge tubes. DNA was extracted with FastDNA™ SPIN Kit for Soil (MP Biomedical) according to the manufacturer's instructions. The total DNA concentration was determined by NANO DROP 2000 (Thermo Scientific) at 260 nm wavelength and the DNA was stored at −80°C until further analysis.

The DNA-SIP gradient fractionation was performed by following the protocol described previously (Jia & Conrad, 2009; Neufeld, Vohra, et al., 2007). In brief, about 2.0 μg of particle-attached or free-living bacterial DNA at day 30 was mixed with Gradient Buffer (GB) and CsCl to achieve a buoyant density of 1.725 g/ml. After symmetry and balance, the mixtures in the ultracentrifuge tube were centrifuged at 190,000 g at 20°C for 44 hr. After centrifugation,

each gradient was fractionated from the bottom of the tube using a peristaltic pump operating at 380 μl/min on continuous mode to collect 14 fractions (~380 μl each). The refractive index of the 14 DNA gradient fractions was measured using AR200 digital refractometer (Reichert, Inc.). Each DNA gradient fraction was purified and then dissolved in 30 μl sterile ddH₂O (Jia & Conrad, 2009; Neufeld, Vohra, et al., 2007), and preserved at −20°C until subsequent treatment.

2.5 | Real-time quantitative PCR

The copy number of bacterial 16S rRNA gene in the 3th-14th fractionated DNA of PAM and FLM was determined on a CFX 96 Optical Real-Time Detection System (Bio-Rad Laboratories Inc.). DNA samples were amplified using primer set Bac331F (5′-TCCTACGGGAGGCAGCAGT-3′) and 797R (5′-GGACTACCAGGGTCTAATCCTGTT-3′) (Nadkarni, Martin, Jacques, & Hunter, 2002). Each 20-μl reaction system contained 1 μl DNA template, 0.3 μl of each primer (0.5 μM), 10 μl SYBR Premix Ex Taq™ (Takara Biotech, Dalian, China), and 8.4 μl sterile ddH₂O. Each sample was performed in triplicate. The qPCR amplification condition was as follows: initial denaturation (95°C) for 30 s; 40 cycles of denaturation (95°C) for 5 s, annealing at 55°C for 30 s, and extension at 72°C for 1 min. The construction of standard curves (Ct value vs. gene copy number) was performed with plasmids DNA including amplicon fragment of Bac27F/1492R. The amplification efficiency of the bacterial 16S rRNA gene was around 100% and the R^2 was <.99.
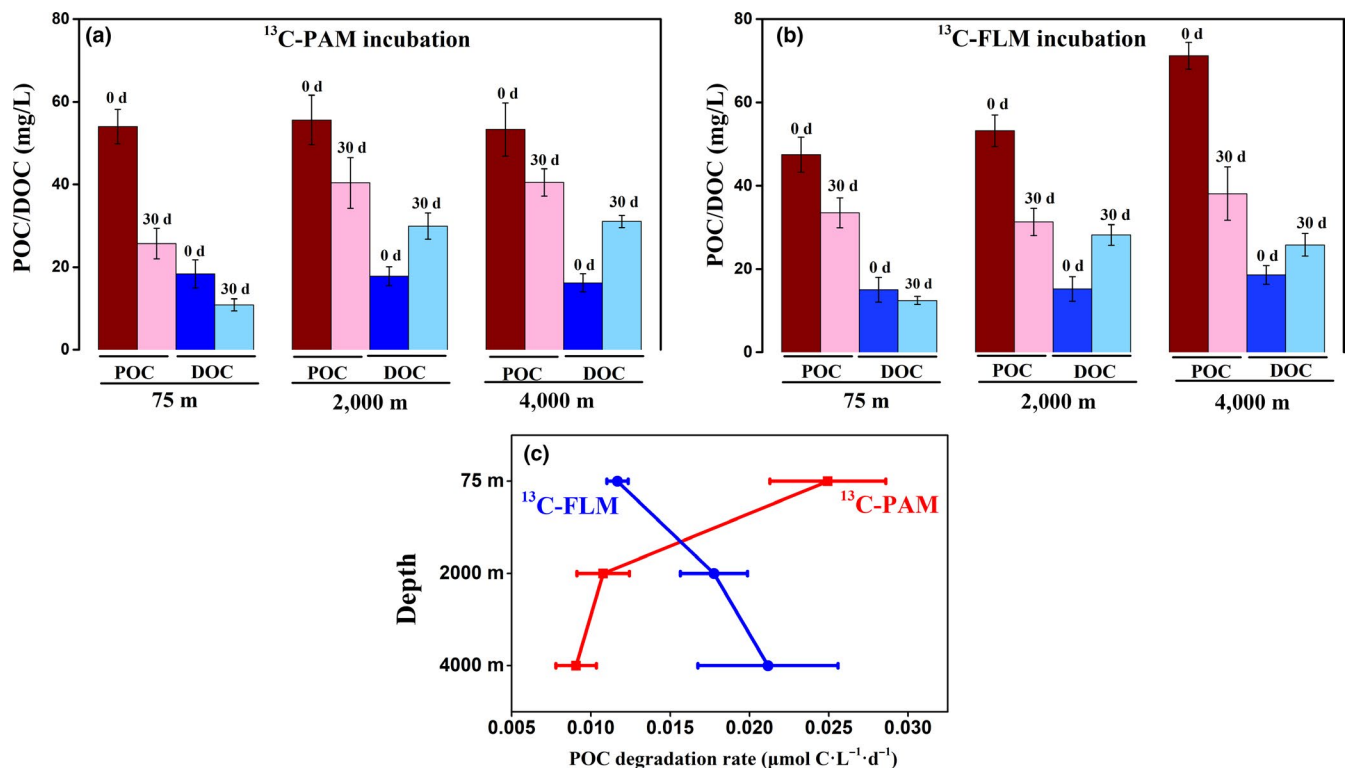
FIGURE 1 Variations of POC and DOC concentrations in PAM (a) and FLM (b) cultures, and POC degradation rates (c) of PAM and FLM incubated with ^{13}C-POC at 0.1, 20, and 40 MPa and 15°C at day 0 and day 30

2.6 | Illumina MiSeq sequencing

Before Illumina high-throughput sequencing, DNA from PAM and FLM at day 0 and the 4th-10th layers of the DNA gradient fractions at day 30 were amplified using the primer pair 515F (5′-GTGCCAGCMGCCGCGG-3′) and 907R (5′-CCGTCAATTCMTTTRAGTTT-3′) (Lane, 1991; Stubner, 2002), targeting the V4-V5 regions of the bacterial 16S rRNA gene. The 12 bp unique barcode sequences that were adhered to the 5′ end of 515F were used to demultiplex sequences. The 50-μl PCR amplification system was conducted in triplicate, with each containing 2.5 μl of DNA template, 1 μl of each primer (10 μM), 25 μl Premix Taq^{TM} (Takara), and 20.5 μl sterile ddH$_2$O. The PCR amplification conditions were as follows: 94°C for 5 min; 32 cycles of 94°C for 30 s, 55°C for 30 s, and 72°C for 45 s; 72°C for 8 min. All PCR amplicons were visualized on 1% (w/v) agarose gels, then pooled and purified using E.Z.N.A Cycle Pure Kit (OMEGA bio-tek). Finally, the purified DNA was quantified by QuantiFluor^{TM}-ST (Promega). The sequencing of purified DNA samples was performed with an Illumina MiSeq platform (Illumina) at the Institute of Soil Science, Chinese Academy of Sciences, Nanjing, China.

The raw high-throughput sequencing data were processed using Quantitative Insights Into Microbial Ecology (QIIME version: 1.9.1) to filtrate effective reads (Caporaso et al., 2010; http://www.qiime.org) with default parameters. The optimizing reads were clustered to operational taxonomic unit (OTU) with a cutoff value of 97% similarity using UPARSE (version 7.1). The representative sequences of OTUs were aligned using the Ribosomal Database Project (RDP) classifier (http://rdp.cme.msu.edu/) against the Silva16S rRNA database (SSU123) (www.arb-silva.de/) using a confidence threshold of 70%.

2.7 | Statistical analysis

To analyze the α-diversity (Shannon, Simpson, Coverage, Ace and Chao) of PAM and FLM communities, all samples in the OTU table were subsampled to the same number of sequences based on the fewest sequences (n = 4,099) using QIIME software (Caporaso et al., 2010; http://www.qiime.org). The variations of shared and unique OTUs in PAM and FLM were calculated by using Venny 2.1 (http://bioinfogp. cnb.csic.es/tools/venny/index.html). Nonmetric multidimensional scaling (NMDS) analysis was used to evaluate the dissimilarity of different samples based on the Bray-Curtis similarity matrix using the software R program (v3.2.3) with vegan package (Pinheiro, Bates, Debroy, Sarkar, & Team, 2012). The analysis of similarity (ANOSIM) was used to test the dissimilarity between samples. The heatmap plot was performed by Heatmap Illustrator 1.0 software (http://hemi.biocuckoo.org/down. php). Phylogenetic tree of the active OTUs in PAM and FLM was constructed through neighbor-joining methods with 1,000 bootstrap values using MEGA 7.0 software (Kumar, Stecher, & Tamura, 2016).

In our study, the active OTUs are defined as those with relative abundance ≥1% that the abundance of an OTU in the ^{13}C-heavy DNA fraction minus the corresponding abundance in the ^{12}C-heavy DNA fraction in PAM and FLM after incubation (Orsi et al., 2016).

3 | RESULTS

3.1 | POC decomposition and DOC degradation

Microbial decomposition and degradation of POC and DOC resulted in drastic changes in concentrations of POC and DOC in the cultures (Figure 1 and Table A2). For PAM cultures, the reduction of POC
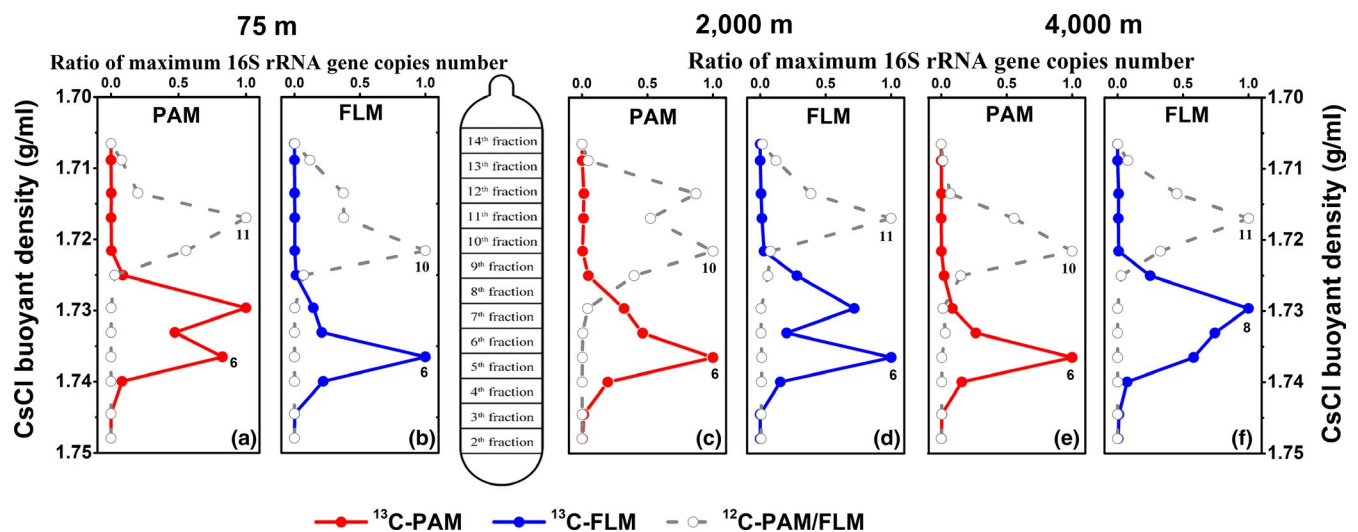
FIGURE 2 The quantitative distribution of the 16S rRNA gene in the 3th-14th DNA fractions across the different buoyant density gradients of the PAM and FLM assemblages incubated with ^{13}C- or ^{12}C-POC at 0.1, 20, and 40 MPa and 15°C for 30 days. (a) 0.1 MPa-PAM; (b) 0.1 MPa-FLM; (c) 20 MPa-PAM; (d) 20 MPa-FLM; (e) 40 MPa-PAM; (f) 40 MPa-FLM. The x-axis represents the ratio of the gene copy number in each DNA fraction to the maximum gene copies in each treatment, according to the previous method (Lueders, Manefield, & Friedrich, 2004). The y-axis represents the variations of CsCl buoyant density in the 3th-14th DNA fractions. The numbers 6 and 8 indicate the ^{13}C-labeled "heavy" DNA fractions while the numbers 10 and 11 show the ^{12}C-labeled "light" DNA fractions

concentrations decreased with pressure, averaging 52% (from 54.0 to 25.7) in the 0.1-MPa culture, 27% (55.6 to 40.4) and 24% (53.3 to 40.5 mg/L) in the 20- and 40-MPa-PAM cultures, respectively (Figure 1a). The FLM cultures showed a slightly different pattern, POC concentrations decreased by 29% (0.1 MPa), 41% (20 MPa), and 46% (40 MPa) (Figure 1b). On the other hand, the concentrations of DOC in PAM and FLM cultures decreased in the 0.1-MPa, and increased in the 20-MPa and 40-MPa (Figure 1a and b).

Biodegradation rates by PAM and FLM assemblages were calculated based on the incorporation of ^{13}C into microbial biomass as described by Suroy, Panagiotopoulos, Boutorh, Goutx, and Moriceau (2015). The POC degradation rates by PAM ranged from 0.009 to 0.025 µmol C L^{-1} day^{-1} at the three pressures, with the maximum rate at atmospheric pressure (Figure 1c). POC degradation rates by FLM were relatively higher, ranging from 0.012 to 0.021 µmol C L^{-1} day^{-1}, with the maximum rate at high pressure (40 MPa). Thus, POC
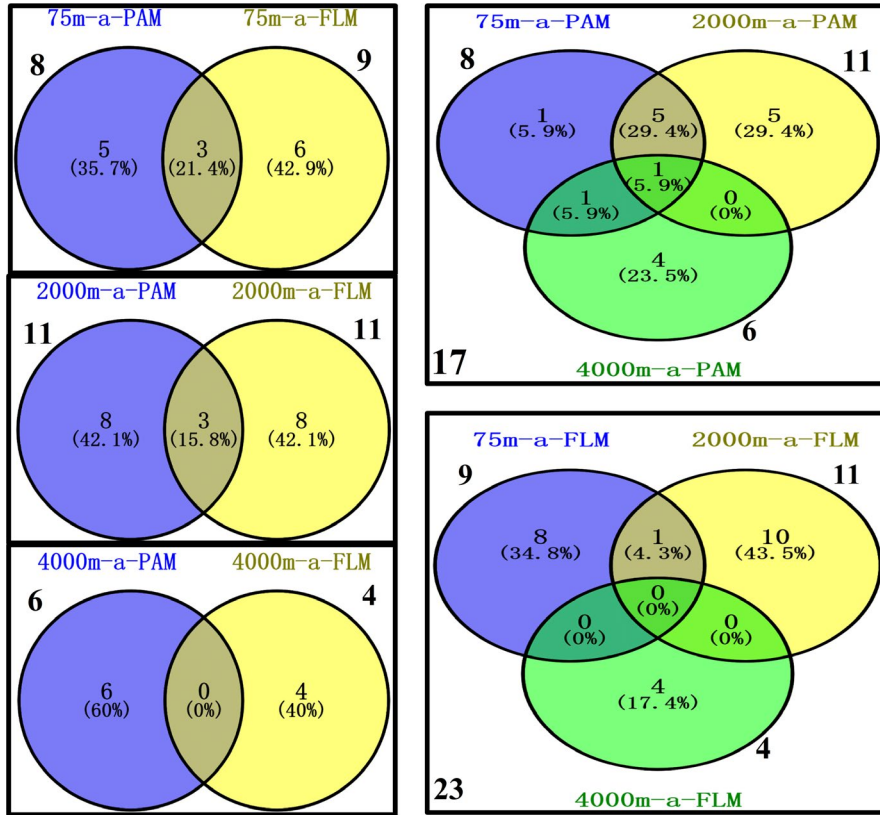
FIGURE 3 Venn diagrams showing the number and percentage of shared or unique active OTUs for PAM and FLM assemblages incubated at 0.1, 20, and 40 MPa and 15°C. Abbreviation: a, active. The numbers in bold are the number of total OTUs in the PAM and FLM assemblages at the three pressures
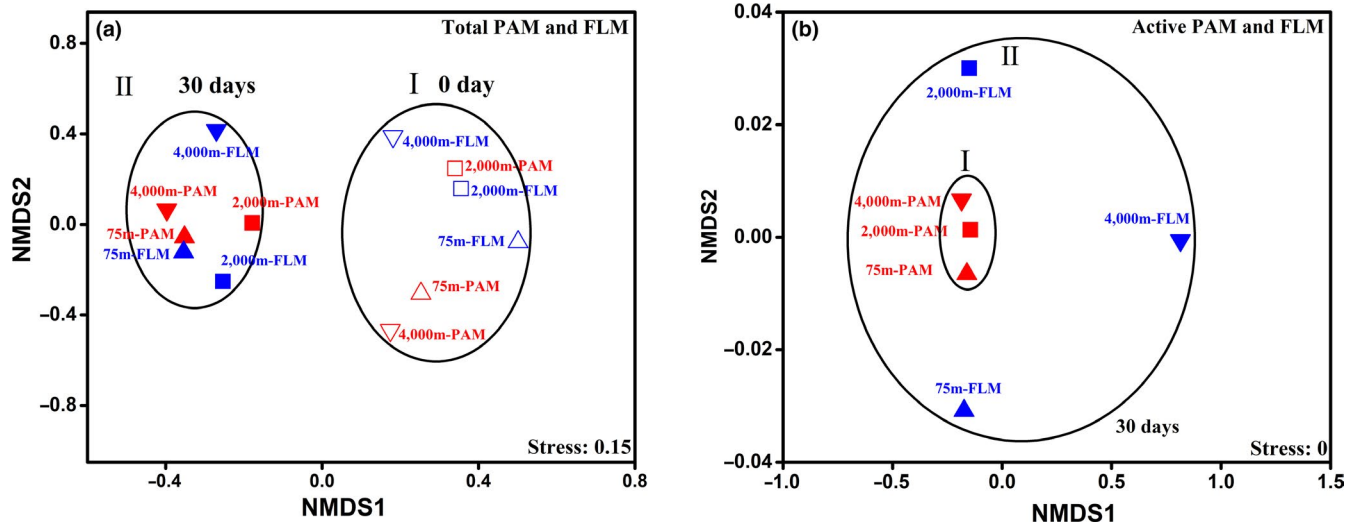
FIGURE 4 Nonmetric multidimensional scaling (NMDS) analysis of the total (a) and active (b) PAM and FLM communities incubated with ^{13}C-POC at 0.1, 20, and 40 MPa and 15°C at day 0 and day 30 based on Bray-Curtis similarity matrix at the OTU level. Different symbols and colors indicate various samples

TABLE 1 Analysis of similarity (ANOSIM) between the PAM and FLM assemblages at 0.1, 20, and 40 MPa and 15°C at day 0 and day 30

ANOSIM				R value	P value
Comparison 1	Total OTUs	Day 0	PAM vs. FLM	.1481	.391
Comparison 2	Total OTUs		Epipelagic (75 m) vs. Bathypelagic (2,000–4,000 m)	.5	.075
Comparison 3	Total OTUs		Day 0 vs. Day 30	.6583	.003
Comparison 4	Total OTUs	Day 30	PAM vs. FLM	.0741	.384
Comparison 5	Total OTUs		75 m vs. 2,000–4,000 m	.3214	.292
Comparison 6	Active OTUs		PAM vs. FLM	0	.529
Comparison 7	Active OTUs		75 m vs. 2,000 m	.5	.338
Comparison 8	Active OTUs		75 m vs. 4,000 m	.25	.32
Comparison 9	Active OTUs		2,000 m vs. 4,000 m	.125	.346

Note: The R value indicates differences between the two groups, while the p value shows the level of significant difference.

FIGURE 5 The relative abundance of the most active PAM and FLM (≥1%) at the phylum (class) level for POC decomposition at 0.1, 20, and 40 MPa and 15°C for 30 days. The x-axis represents the increased relative abundance, that is, the abundance of a phylum (class) in the ^{13}C-labeled "heavy" DNA fraction minus the corresponding abundance in the ^{12}C-labeled "heavy" DNA fraction at day 30
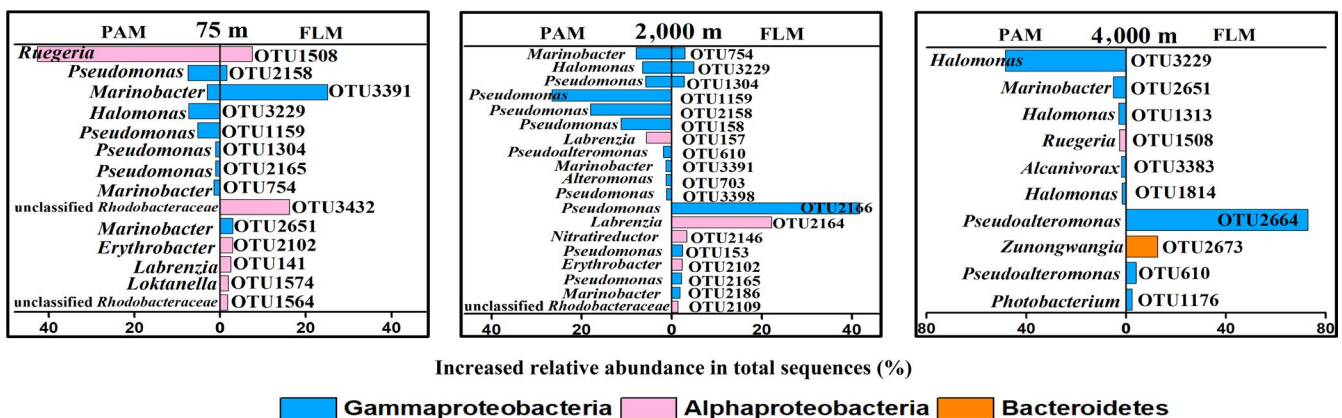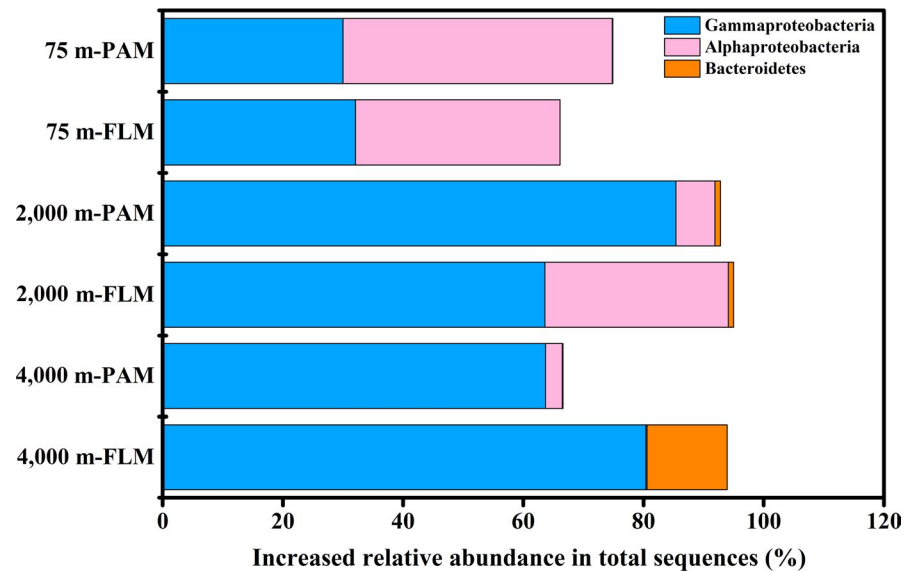
FIGURE 6 The relative abundance of the most active genera (OTUs) (≥1%) in the PAM and FLM assemblages for POC decomposition at 0.1, 20, and 40 MPa and 15°C for 30 days

degradation rates by the PAM communities decreased markedly with pressure, whereas POC degradation rates by the FLM communities increased with pressure (Figure 1c). Overall, POC degradation rates were much higher at atmospheric pressure than that at high pressure at 15°C (Figure 1c).

Furthermore, the variations in δ^{13}C values of POC showed that the percentage of ^{13}C-labeled substrate (the atom percent of ^{13}C) utilized by the PAM and FLM were 4.2 and 2.6%, 2.1 and 2.2%, and 1.2 and 3.5% at 0.1, 20, and 40 MPa under 15°C, respectively (Table A3).
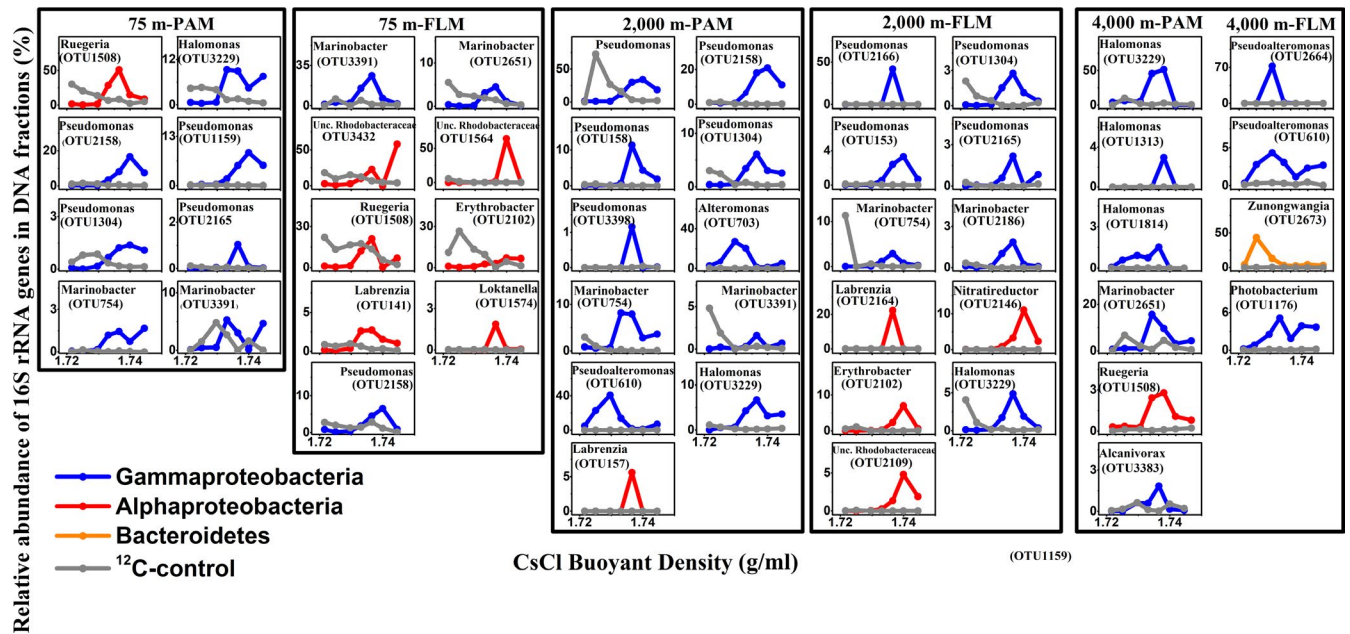
FIGURE 7 The relative abundance of active OTUs for POC decomposition in the 4th-10th DNA fractions across the different buoyant density gradients from ^{13}C-labeled (green, red, and blue solid lines) and ^{12}C-control (gray solid lines) groups in the PAM and FLM assemblages incubated at 0.1, 20, and 40 MPa and 15°C for 30 days
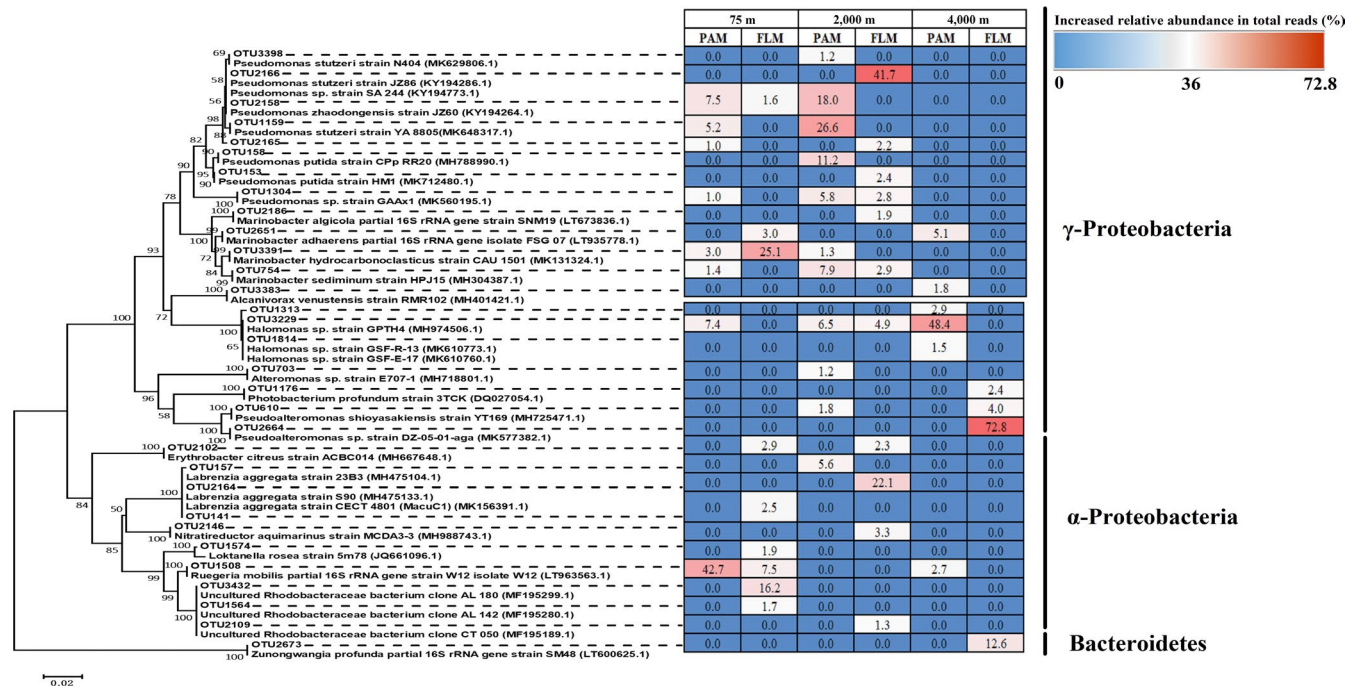
FIGURE 8 Phylogenetic tree of active PAM and FLM OTUs at 0.1, 20, and 40 MPa and the most matched sequences in the NCBI database after 30-day incubation. The tree was constructed by neighbor-joining method with Mega (7.0). The Bootstrap method is 1,000 Bootstrap replicates, and values higher than 50% are shown at the nodes. The relative abundance of active OTUs in PAM and FLM at 0.1, 20, and 40 MPa was shown at right

3.2 | Identifying PAM and FLM that utilized POC

Results of real-time quantitative PCR showed that the maximum copy number of bacterial 16S rRNA gene appeared in the 6th or 8th "heavy" DNA fractions of the PAM- and FLM-^{13}C cultures (Figure 2), with the maximum value of 5×10^6 copies/ml in ^{13}C-PAM culture

at 0.1 MPa, while the bacterial abundance peaked in the 10th or 11th "light" fractionated DNA for ^{12}C-control treatment, with the highest value of 1.2×10^7 copies/ml in ^{12}C- FLM culture at 0.1 MPa (Table A4). The bacterial copy number in ^{13}C-PAM culture was higher than that of ^{13}C-FLM culture at 0.1 and 40 MPa, whereas the bacterial copy number of PAM was lower than that of FLM at

20 MPa (Table A4). The CsCl buoyant density (BD) shift, defined as the difference in buoyant density between the (^{13}C-^{12}C) peak layers, ranged from 0.013–0.02 g/ml in PAM and FLM at three different pressures, with the highest in the ^{13}C-PAM culture at 0.1 MPa and ^{13}C-FLM culture at 20 MPa, and lowest in the ^{13}C-FLM culture at 40 MPa (Table A5).

By Illumina sequencing, a total of 2,112,639 high-quality reads in 90 samples were obtained with an average length of 421 bp. The reads were clustered into 3,533 operational taxonomic unit (OTU) based on 97% sequence similarity. Alpha-diversity index showed that the diversity index (Shannon and Simpson) of PAM and FLM decreased markedly after cultivation. However, the microbial richness (Ace and Chao) and diversity (Shannon and Simpson) between PAM and FLM were similar in day 30 (Table A6 and Figure A2).

The Venn diagrams indicate that before incubation, a total of 771 and 244 OTUs were identified in the PAM and FLM assemblages, respectively. Around 452, 118, and 498 OTUs in the PAM fraction were distributed at 75-, 2,000-, and 4,000-m depths, respectively. Correspondingly, only 142, 92, and 58 OTUs in the FLM fraction were identified at 75, 2,000, and 4,000 m depths (Figure A3). However, after 30-d cultivation, only 17 and 23 active OTUs were identified in PAM and FLM fractions, with 8, 11, and 6 active OTUs for PAM, and 9, 11, and 4 active OTUs for FLM at 0.1-, 20-, and 40-MPa pressures, respectively (Figure 3). At day 0, the OTUs of PAM only, FLM only, and the transient form (occurs in both the PAM and FLM fractions) were 405, 47, and 95 for 75-m culture, respectively; the unique OTUs of PAM, the unique OTUs of FLM, and the shared OTUs between the PAM and FLM were 64, 54, and 38 for 2,000-m culture, respectively; and only PAM OTUs, only FLM OTUs, and the common OTUs of PAM and FLM were 456, 42, and 16 for 4,000-m culture, respectively (Figure A3). After 30-days incubation, the corresponding number of active OTUs were reduced to 5, 3, 6; 8, 3, 8; and 6, 0, 4 (Figure 3). Among 31 OTUs, 8 and 14 OTUs existed exclusively as PAM and FLM, respectively, and 9 as transient form (Table A7).

The nonmetric multidimensional scaling (NMDS) analysis was performed to compare the similarities between PAM and FLM at 0.1, 20, and 40 MPa and 15°C before and after incubation (Figure 4a). Two clusters were formed: the PAM and FLM in day 0 (I) and day 30 (II), suggesting significant dissimilarity in microbial communities before and after incubation (Figure 4a). Analysis of similarity (ANOSIM) also revealed significant differences in microbial communities between day 0 and day 30 ($R = .6583$, $p = .003$, Table 1). The active PAM and FLM for POC decomposition at 0.1, 20, and 40 MPa and 15°C in day 30 also formed two clusters, active PAM (I), and active FLM (II) (Figure 4b). However, ANOSIM analysis ($R = 0$, $p = .529$, Table 1) revealed much less differences between the two.

Before incubation, the PAM assemblage was dominated by Gammaproteobacteria (genus *Pseudoalteromonas*) and Alphaproteobacteria (genus *Erythrobacter*), Alphaproteobacteria (Rhodobiaceae) and Gammaproteobacteria (genus *Marinobacter*), and Gammaproteobacteria (genus *Amphritea*) and Actinobacteria

(genus *Propionibacterium*) at 75-, 2,000-, and 4,000-m depths, respectively (Figures A4 and A5). The preincubation FLM assemblages were dominated by Gammaproteobacteria (genus *Alcanivorax*) and Alphaproteobacteria (genus Surface 1), Bacteroidetes (genus *Polaribacter 4*) and Gammaproteobacteria (genus *Alcanivorax*), and Gammaproteobacteria (genus *Alcanivorax*) at 75-, 2,000-, and 4,000-m depths, respectively (Figures A4 and A5). Archaea had an abundance of <1% (data not shown) and will not be discussed thereafter.

After the 30-day incubation, the PAM communities responsible for POC utilizing were dominated by Alphaproteobacteria (genus *Ruegeria*) and Gammaproteobacteria (genera *Pseudomonas* and *Halomonas*) in the 0.1-MPa culture, Gammaproteobacteria (genera *Pseudomonas*, *Marinobacter* and *Halomonas*) and Alphaproteobacteria (genus *Labrenzia*) in the 20-MPa culture, and Gammaproteobacteria (*Halomonas* and *Marinobacter* genera) in the 40-MPa communities (Figures 5 and 6). On the other hand, the active FLM community was dominated by Gammaproteobacteria (*Marinobacter*) and Alphaproteobacteria (unclassified Rhodobacteraceae and *Ruegeria*), Gammaproteobacteria (*Pseudomonas*) and Alphaproteobacteria (*Labrenzia*), and Gammaproteobacteria (*Pseudoalteromonas*) and Bacteroidetes (*Zunongwangia*) in the 0.1-, 20-, and 40-MPa cultures, respectively (Figures 5 and 6).

Thirty-one active OTUs responsible for POC decomposition were identified in PAM and FLM assemblages after 30 days (Figures 7 and 8 and Table A8). These active OTUs were affiliated with 14 genera in three classes: Gammaproteobacteria, Alphaproteobacteria, and Flavobacteria (Table A8). The relative abundance of dominant active OTUs in the 4th-10th fractionated DNA along the different buoyant density gradients can be seen in Figure 7. This result indicates that the relative abundance of each OTU was much higher in the "heavy" fractionated DNA of the ^{13}C-labeled treatment than the corresponding abundance in the ^{12}C-control treatment (Figure 7). It also revealed that these active microorganisms had sufficient cell division and incorporated enough ^{13}C-labeled POC into cell biomass, for detection by DNA-SIP. Phylogenetic analysis (Figure 8) showed that the similarity of each OTU sequence could reach up to 99%–100% when aligned in the NCBI database, which implies that most of the marine microbes involved in POC decomposition and utilization were known microbial strains.

As shown in the hierarchically clustered heatmap, the active OTUs decomposing POC in PAM and FLM incubated at three different pressures and 15°C formed two distinct clusters; one for PAM and FLM incubated at atmospheric pressure (0.1 MPa), and the other for PAM and FLM incubated at high pressures (20 and 40 MPa) (Figure A6). We found that members of Alphaproteobacteria and Gammaproteobacteria were mainly responsible for POC decomposition at atmospheric pressure, whereas microbial taxa affiliated with Gammaproteobacteria predominated POC decomposition at high pressures (Figure 5). The relatively high proportion of *Ruegeria* (Alphaproteobacteria) appeared at atmospheric pressure in particle-associated fraction (42.9% of the total sequences), and their
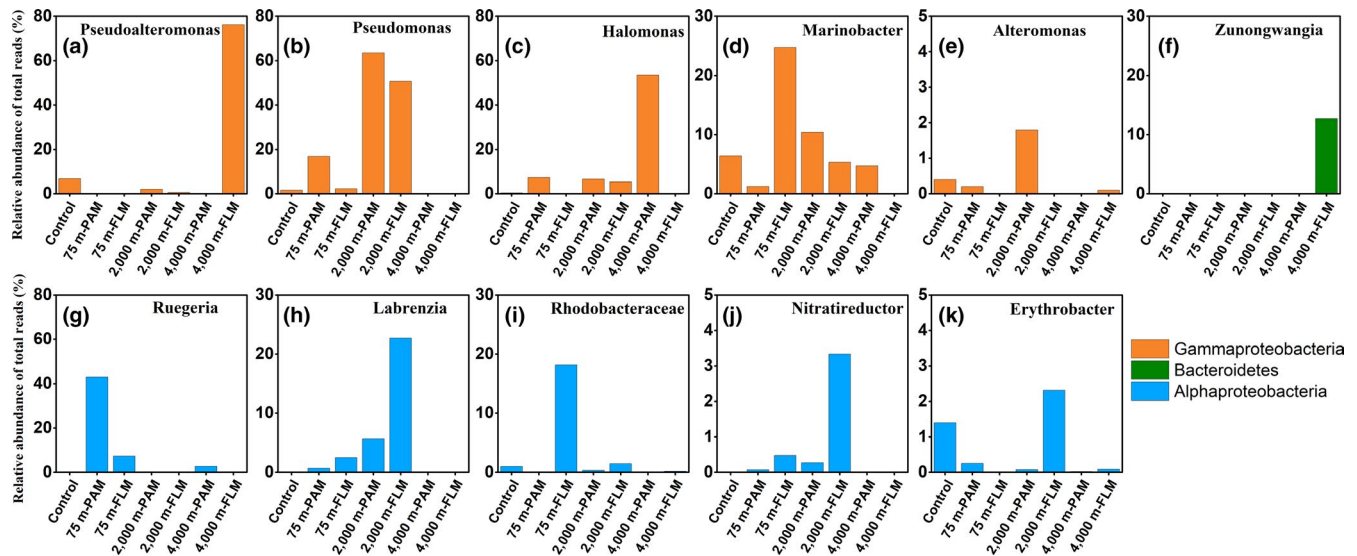
FIGURE 9 The relative abundance of active particle-attached and free-living microbial taxa for POC decomposition incubated at 0.1, 20, and 40 MPa and 15°C for 30 days. (a–e) members of Gammaproteobacteria; (f) member of Bacteroidetes; (g–k) members of Alphaproteobacteria. The control indicates the relative abundance of the same genus in the original seawater (day 0)

abundance decreased sharply with pressure. Similarly, *Marinobacter* showed much higher relative abundance at 0.1 MPa than at high pressures, with the maximum value of 24.7% in the free-living fraction. *Pseudomonas* was the most abundant taxa for POC decomposition at 20 MPa pressure in the particle-attached (63.5%) and free-living (50.7%) fractions. In addition, *Labrenzia*, *Nitratireductor*, *Erythrobacter* were the dominant genera at 20 MPa in the free-living fraction, with the relative abundances of 22.7%, 3.3%, and 2.3%, respectively (Figure 9). At 40 MPa, *Pseudoalteromonas* (76.2%) and *Zunongwangia* (12.7%) were the most dominant free-living taxa utilizing POC while *Halomonas* (53.6%) were the most abundant bacterial taxon assimilating POC in particle-attached fraction (Figure 9).

4 | DISCUSSION

Diatom-derived detrital particles form a vertical POM-DOM continuum (Azam, 1998; Fang et al., 2015; Grossart, 2010; Verdugo et al., 2004) and provide important nutrient- and carbon-rich hotspots for the growth and metabolism of heterotrophic prokaryotes (Azam & Long, 2001), from the surface waters to the bathypelagic zones in the ocean. Here, we investigated the specific bacterial lineages actively participated in the POC decomposition and DOC degradation at low and high pressures under 15°C condition, and demonstrated that most of the active microbial taxa were those previously detected in organic particle decomposition and utilization.

4.1 | POC decomposers, PAM or FLM?

Our results revealed that not only PAM, but also FLM decomposed diatom-derived POC and assimilated the released DOC at low and high pressures under 15°C conditions (Figures 1, 5, and 6). These

results further support a previous hypothesis that PAM almost immediately attached to organic particles and secreted exoenzyme to hydrolyze POC and produce DOC (Azam & Long, 2001; Fang et al., 2015; Grossart, Tang, Kiørboe, & Ploug, 2007; Kiørboe & Jackson, 2001; Smith et al., 1992). It is important to note that, due to motility (Grossart, 2010; Grossart & Ploug, 2001) and chemotaxis (Kiørboe, Grossart, Ploug, & Tang, 2002), the FLM assemblages were also able to attach to diatom detrital particles, and produce extracellular enzyme (Grossart et al., 2007) to decompose POC and take advantage of the released DOC when PAM was absent (Figure 1). These results suggest that microbial lifestyles (i.e., particle-attached and free-living) were not strictly correlated with their ecological functions, different from the original hypothesis: PAM for decomposing POC and FLM for degrading the released DOC (Azam & Long, 2001; Fang et al., 2015; Kiørboe & Jackson, 2001). These findings also added to our current understanding that either particle-associated microorganisms (Karl et al., 1988) or free-living microorganisms (Cho & Azam, 1988) were responsible for POC decomposition.

Our DNA-SIP results revealed that POC decomposition was accomplished by members of Gammaproteobacteria, Alphaproteobacteria, and Bacteroidetes at low and high pressures (Figure 5), in agreement with findings in previous studies that these microbial taxa had the specialized capability in decomposition of phytoplankton-derived organic matter (e.g., Buchan, LeCleir, Gulvik, & González, 2014; Mayali, Stewart, Mabery, & Weber, 2016; Orsi et al., 2016; Tamburini et al., 2006; Teeling et al., 2012).

Even though the original PAM communities differed greatly from the FLM communities at phylum- or genus-level (Figures A4 and A5), much more similar microbial taxa, of both PAM and FLM, actively participated in POC decomposition (Figure 4b and Table 1). For instance, in the PAM fraction, the microbial POC decomposers were mainly affiliated with *Ruegeria* (43%, 0.1 MPa), *Pseudomonas* (63%, 20 MPa), and *Halomonas* (53%, 40 MPa) (Figure 6). Similarly, the FLM

microbial taxa that mediated POC decomposition and degradation were dominated by *Marinobacter* (28%, 0.1 MPa), by *Pseudomonas* (49%, 20 MPa), and by *Pseudoalteromonas* (77%, 40 MPa) (Figure 6). This result suggests the functional commonality of microbial communities of the two lifestyles (i.e., PAM and FLM) under the conditions of this work (15°C temperature and high concentrations of substrates) (Ghiglione, Conan, & Pujopay, 2009; Hollibaugh, Wong, & Murrell, 2000; Liu, Wang, et al., 2018; Riemann & winding, 2001).

Our results indicated that most of the active microbial taxa involved in POC decomposition were dominated in either the particle-attached or free-living mode (Table A7). We hypothesize that switching of lifestyles (particle-attached vs. free-living) reflects microbial adaptation to the changing environmental conditions (e.g., hydrostatic pressure; Ghiglione et al., 2007; Moeseneder, Winter, & Herndl, 2001) and/or seeking and utilization of growth substrates (e.g., Lauro et al., 2009). For instance, the copiotrophic *Marinobacter* occurred in both PAM and FLM fractions and changed their lifestyle from the free-living state at atmospheric pressure to particle-attached at high pressure, and became undetectable in the FLM fraction at 40 MPa (Figure 9). This result supports the notion that a particle-attached lifestyle may be preferentially selected by deep-sea microorganisms (DeLong et al., 2006; Herndl & Reinthaler, 2013; Liu, Wang, et al., 2018). On the other hand, the four active Alphaproteobacterial taxa, *Labrenzia*, Rhodobacteraceae, *Nitratireductor*, and *Erythrobacter* that assimilated ^{13}C-labeled POC seem to be presented nearly exclusively in free-living lifestyle, as do *Pseudoalteromonas* and *Zunongwangia* (Figure 9).

Our data also showed that only 7% of PAM and 10% of FLM OTUs were actively involved in POC decomposition and remineralization processes (Table A7). However, on average, 34% and 52% of the total sequences appeared in active PAM and FLM OTUs, respectively, with the overlap fractions reaching up to 31% in the two size fractions (Table A7), suggesting that particle-attached and free-living microbial communities were interacting assemblages, with active succession of lifestyles between the two (Ghiglione et al., 2009; Riemann & Winding, 2001). Our results accord with previous studies that showed high proportions of shared OTUs between PAM and FLM in the euphotic waters (25%, Crespo, Pommier, Fernández-Gómez, & Pedrós-Alió, 2013), mesopelagic waters (30%, Moeseneder et al., 2001), and bathy- and abyssopelagic waters (82%, Liu, Wang, et al., 2018).

At the OTU level, the representative OTU 1508 affiliated with *Ruegeria* genus assimilated more ^{13}C-POC than other 7 OTUs in the PAM fraction at 0.1 MPa, with the relative abundance of 43% and BD shift of 0.02 g/ml (Figures 7 and 8), implying that *Ruegeria* probably playing an important role in POC decomposition (Reisch et al., 2013; Reisch, Moran, & Whitman, 2011). In contrast, the most abundant active OTU 3391, affiliated with *Marinobacter* and known for being able to degrade algae exudate (Nelson & Carlson, 2012), was responsible for POC decomposition in the FLM fraction at 0.1 MPa and accounted for 25% of the total sequences, with BD shift of 0.015 g/ml (Figures 7 and 8). OTU1159 and OTU2166 from the marine bacteria *Pseudmonas* were the most dominant and active taxa for POC

incorporated in both particle-attached and free-living bacterial communities at 20 MPa, with the relative proportion of 27% and 42%, respectively (Figures 7 and 8). Our results are apparently different from a previous report which showed that the *Pseudomonas* species have limited ability to degrade high molecular weight organic matter (Fukami, Simidu, & Taga, 1981). OTU 3229 affiliated with *Halomonas* genus was the most dominant taxon for utilizing POC in particle-associated fraction at 40 MPa, constituting 49% of the total reads, whereas OTU2664 affiliated to *Pseudoalteromonas* was the most abundant group for decomposing POC exclusively in the free-living fraction, with a percentage of 73% (Figures 7 and 8). The BD shifts of active OTU3229 and OTU2664 were 0.015 and 0.013 g/ml for particle-associated and free-living bacteria at 40 MPa, respectively, much less than that at 0.1 and 20 MPa (Figure 7). By NCBI blast, we found that the OTU2664 had 100% similarity to *Pseudoalteromonas* sp. strain DZ-05-01-aga (MK577382.1) (Figure 8), an isolate which was identified as a macroalgae–polysaccharide-degrading bacterium (Martin et al., 2015). It has been shown that *Pseudoalteromonas* can produce a large number of ectoenzymes to hydrolyze POC (Chen, Zhang, Gao, & Luan, 2003; Qin et al., 2011) and high molecular weight DOC (Alonso & Pernthaler, 2005; Covert & Moran, 2001; Nelson & Carlson, 2012).

It seems likely that POC decomposition was mediated mainly by members of the "rare biosphere" (Sogin et al., 2006), those that were of a rather low abundance in the epi- and bathypelagic waters of the NBT (Ghiglione et al., 2007, 2009). For instance, the bacterial taxon Ruegeria (0% of the total community in day 0 vs 43% of the active community in day 30) at 0.1 MPa, Pseudomonas (2% vs. 63%) at 20 MPa, and Halomonas (0% vs. 53%) and Pseudoalteromonas (7% vs. 77%) at 40 MPa (Figure 6 and Figure A5). It is also possible that our incubation conditions favored microbes that prefer nutrient-rich environments (i.e., copiotrophs).

4.2 | Effects of pressure and temperature on POC decomposition rates

Particulate organic carbon degradation rates of PAM and FLM were remarkably affected by hydrostatic pressure, that is, POC decomposition was accomplished primarily by PAM communities at atmospheric pressure and by FLM at high pressures (20 and 40 MPa) and temperature of 15°C (Figure 1 and Table A2). It has been assumed that the PAM assemblages had higher metabolic rates and extracellular enzyme activities than FLM in organic carbon remineralization at atmospheric pressure, which had also been observed in previous studies in the surface ocean (Fandino, Riemann, Steward, Long, & Azam, 2001; Grossart et al., 2007; Herndl & Reinthaler, 2013; Lapoussière, Michel, Starr, Gosselin, & Poulin, 2011). Recent reports claimed that the particle-attached microorganisms in the deep ocean originated from the surface water by adhering to the sinking particles (Duret, Lampitt, & Lam, 2019; Mestre et al., 2018; Thiele, Fuchs, Amann, & Iversen, 2015). When these heterotrophic

prokaryotes reached to the deep ocean along with sinking particles, their extracellular enzyme activity declined significantly with elevated pressure (Liu, Fang, et al., 2018; Tamburini et al., 2006); therefore, POC degradation rate by PAM at atmospheric pressure was usually higher than that at high pressure (Tamburini et al., 2013). On the other hand, free-living bacteria, the in situ colonizers of the deep ocean, may show optimal metabolic activity for POC decomposition and remineralization under high pressure (Dang & Lovell, 2016; Lauro & Bartlett, 2008). Thus, POC degradation rates by deep-sea FLM were generally higher than by PAM. In addition, some previous studies noted that particle-attached bacteria were typical copiotrophs which can grow rapidly under high nutrient conditions such as nutrient-enriched particles in the surface waters, whereas free-living bacteria were oligotrophs that may adapt better to the bathypelagic realm (Herndl & Reinthaler, 2013; Lauro et al., 2009).

Furthermore, variations of DOC concentrations showed that DOC concentrations decreased at low pressure (0.1 MPa) and increased at high pressures (20 and 40 MPa) (Figure 1), suggesting that DOC utilization by PAM and FLM was likely less efficient at higher pressures than at atmospheric pressure under 15°C condition. These results also revealed that microbial decomposition of POC was accompanied by the release of DOC, and that there was a tight coupling between POC decomposition and DOC utilization (Azam & Long, 2001; Fang et al., 2015).

It must be emphasized that in the present study, we set 15°C as the incubation temperature, much higher than the in situ temperature of the deep sea (around 2°C), in order to produce enough biomass for subsequent analysis. Previous studies also reported that increasing incubation temperature generally increased bacterial activity and metabolism, and could significantly improve bacterial growth and carbon utilization (Middelboe & Lundsgaard, 2003; Pomeroy & Wiebe, 2001). Other findings showed that increasing temperature would enhance the adhesive properties of marine microbes (Garrett, Bhakoo, & Zhang, 2008), facilitating bacteria attachment to particles. Elevated temperature may also increase the rate of enzymatic reactions, thus, the hydrolytic activity of ectoenzymes that secreted mainly by particle-attached bacteria can be enhanced (see e.g., Garrett et al., 2008), further increasing the efficiency of microbial decomposition of POC and degradation of DOC (Middelboe & Lundsgaard, 2003). Thus, it is likely that the measured POC degradation rates were higher than the actual rates in the bathypelagic zone of the NBT. Future studies should focus on how temperature affects microbial-mediated POC degradation rates and microbial exoenzymatic activities.

4.3 | Pressure effects on active PAM and FLM communities involved in POC decomposition

Hydrostatic pressure significantly affected particle-attached and free-living microbial communities responsible for POC decomposition and DOC degradation (see Figures 5, 6 and 9, and Figure A6). The microbial communities incubated at atmospheric pressure (0.1 MPa) and high pressures (20 and 40 MPa) formed two distinct clusters (Figure A6).

The members of Gammaproteobacteria (e.g., copiotrophic genera *Halomonas*, *Marinobacter*, and *Pseudoalteromonas*) were mainly POC decomposers at high pressures (20 and 40 MPa) (Figures 5, 6, and 9). Similarly, a series of the latest findings demonstrated that the PAM and FLM communities were dominated by Gammaproteobacteria (e.g., *Colwellia*, *Moritella*, *Shewanella*, *Alteromonas*, *Halomonas*, *Pseudoalteromonas*, and *Marinobacter*) in the bathypelagic zone of the Pacific Ocean (Boeuf et al., 2019), the New Britain Trench (Liu, Wang, et al., 2018) and the global ocean (Salazar et al., 2016), the abyssopelagic zone of the Puerto Rico Trench (Eloe et al., 2011), the bottom waters of the Mariana Trench and the Kermadec Trench (Peoples et al., 2018). Other studies also revealed that high pressure led to the increase in the relative abundance of Gammaproteobacteria in prokaryotic assemblages when incubated with diatom detritus (Tamburini et al., 2006) or sinking fecal pellets (Tamburini et al., 2009), which were consistent with our study.

On the other hand, members of Alphaproteobacteria (genus *Ruegeria*) and Gammaproteobacteria (genus *Marinobacter*) dominated the diatom-associated and free-living POC decomposers at atmospheric pressure (Figures 5, 6, and 9). However, previous reports indicated that particle-attached and free-living bacteria were mainly affiliated with Bacteroidetes, Gammaproteobacteria, and Alphaproteobacteria during diatom or dinoflagellate blooms (Bidle & Azam, 2001; Fandino et al., 2001; Grossart, Levold, Allgaier, Simon, & Brinkhoff, 2005).

Nevertheless, Marietou and Bartlett (2014) investigated the effects of pressure on coastal bacterial community, and reported that the relative abundance of Alphaproteobacteria increased significantly with pressure while Gammaproteobacteria dominated the microbial communities at atmospheric pressure, in opposition to our observations in this study. The microbial communities may be originated from the water column of the open ocean (the NBT), significantly different from those in the California coastal water. Other contributing factors may include the incubation conditions, such as temperature (15°C in our study) and pressure.

The effects of incubation temperature on PAM and FLM communities for POC decomposition must be considered here. It has been demonstrated that temperature plays an important role in shaping the microbial community structure in the ocean. For instance, an investigation showed that the shallow coast-water microbial community formed two distinct clusters when incubated at 3 and 16°C at atmospheric pressure (Marietou & Bartlett, 2014). Therefore, the higher temperature (than in situ) incubations may change the community structure of PAM and FLM. Future studies should investigate how temperature affects the active microbial community structure involved in POC decomposition.

4.4 | Limiting factors for the DNA-SIP approach and caveats of this study

The success of the DNA-SIP method depends on several factors among which incorporation of the isotopically labeled substrate into targeted macromolecules (e.g. DNA, RNA) is critical (Liu, Wawrik, &

Liu, 2017; Radajewski, Mcdonald, & Murrell, 2003). One of the challenges is the incubation times and conditions that mirror the in situ environmental conditions (Neufeld, Wagner, & Murrell, 2007). As microbial DNA replication requires cell division, unlike using PLFA- or RNA-SIP, a successful DNA-SIP experiment requires sufficient cell division in the presence of isotopically labeled substrate for separation of labeled DNA from nonlabeled DNA (Neufeld, Dumont, Vohra, & Murrell, 2007; Neufeld, Wagner, et al., 2007). On the other hand, piezophilic and piezotolerant bacterial growth at in situ temperature and pressure conditions is typically rather slow (Fang et al., 2003, 2006). For these reasons, we added relatively high concentrations of growth substrate and incubated the PAM and FLM for 30 days at in situ pressure, but at 15°C, until early stationary phase, to generate high enough biomass.

Our results showed that sufficient isotopic labeling of nucleic acids relative to unlabeled substrates has been achieved. However, the long incubation time could have likely led to the cross-feeding of metabolic byproducts and microbial community shifts (Neufeld, Dumont, et al., 2007; Wang et al., 2015). Cross-feeding is one of the intercellular interactions among microbes to maintain the stability and ecological functions of microbial communities and can exist in any environment (Pande et al., 2016; Seth & Taga, 2014). Additionally, long incubation time often provides greater isotope incorporation, but at the same time, may result in the bottle effect. Previous work has shown that within a few hours, the bottle effect is seen for microbes (Lee & Fuhrman, 1991). In essence, this and other closely related microbiological interactions (e.g., producers and cheaters in microbial extracellular enzyme production and substrate utilization, Allison & Vitousek, 2005) warrant further exploitation in future DNA- or RNA-SIP studies.

In our experiment, we initially separated the total microbes into the PAM and FLM fractions and incubated the separated microbes with the ^{13}C-labeled and unlabeled diatomic particulates. However, PAM and FLM assemblages were not separated after 30-days incubation. Indeed, there can be microbial successions (attachment and de-attachment to and from the particles) during the incubation. Thus, the specific roles of PAM and FLM in POC decomposition and DOC utilization cannot be exclusively specified in our study. Nevertheless, we used the sensitive SIP method to target both PAM and FLM communities simultaneously and overcome the limitation of their slow growth, to detect the potential primary players in POM decomposition and DOM degradation at low and high pressures under 15°C condition. The high degree of ^{13}C-enrichment, evidenced by the BD shift (0.013–0.02 g/ml) of the fractionated DNA (Table A5) and the ^{13}C-labeled POC utilization by PAM and FLM communities (Table A3), indicates the active ^{13}C incorporation into bacterial DNA.

5 | CONCLUSIONS

By using the DNA-SIP approach, we provided direct evidence that linked specific bacterial taxa to POM decomposition and DOM degradation in the epi- and bathypelagic zones where these processes primarily take place in the ocean. Major conclusions and implications are as follows:

1. A total of 14 active particle-attached and free-living bacterial taxonomic groups that actively participated in decomposition and assimilation of diatom-derived POM were identified. Both the particle-attached and free-living microorganisms were able to decompose POC and assimilate the released DOC.
2. POM decomposition process appears to be significantly influenced by hydrostatic pressure, accomplished primarily by particle-attached microorganisms at atmospheric pressure and by free-living microorganisms at high pressure. Overall, the POC degradation rates were higher at low pressure than at high pressure. However, similar bacterial taxa in both the PAM and FLM assemblages were involved in POC decomposition and DOC degradation, suggesting the decoupling between microbial lifestyles and ecological functions.
3. It appears that the microbial taxa actively involved in POC decomposition and degradation were typical of relatively low abundance among those that can perform the same function in processing organic matter in the pelagic zones, reflecting the functional redundancy of microbial communities in both the surface and deep waters of the ocean. Our study highlights the connectivity between microbial lifestyles (i.e., PA or FL) and POC degradation processes in the ocean.

CONFLICT OF INTEREST
None declared.

AUTHOR CONTRIBUTIONS
Ying Liu: Data curation (lead); formal analysis (lead); investigation (lead); methodology (lead); software (lead); writing-original draft (lead); writing-review & editing (equal); Jiasong Fang: Conceptualization (lead); funding acquisition (lead); project administration (lead); resources (lead); writing-review & editing (equal); Zhongjun Jia: formal analysis (equal); methodology (equal); software (equal); review & editing (equal); Songze Chen: formal analysis (equal); methodology (equal); software (equal); validation (equal); writing-review & editing (equal); Li Zhang: conceptualization (equal); funding acquisition (equal); project administration (equal); Wei Gao: data curation (equal); software (equal); writing-review & editing (equal).

ETHICS STATEMENT
None required.

DATA AVAILABILITY STATEMENT

The raw sequence datasets of the bacterial 16S rRNA gene from this project have been deposited at the National Center for Biotechnology Information (NCBI) Sequence Read Archive (SRA) with accession numbers SRR6027268 to SRR6027351 from DNA-SIP. The nucleotide sequences of 16S rRNA gene of PAM and FLM in the water column of the NBT have been deposited at the NCBI database with accession numbers SRR6031465 to SRR6031470.

ORCID

Ying Liu https://orcid.org/0000-0003-0375-8303

REFERENCES

Allen, E. E., Facciotti, D., & Bartlett, D. H. (1999). Monounsaturated but not polyunsaturated fatty acids are required for growth of the deep-sea bacteriumPhotobacterium profundum SS9 at high pressure and low temperature. *Appl. Environ. Microbiol.*, *65*(4), 1710–1720. https://doi.org/10.1128/AEM.65.4.1710-1720.1999

Allison, S. D., & Vitousek, P. M. (2005). Responses of extracellular enzymes to simple and complex nutrient inputs. *Soil Biology & Biochemistry*, *37*(5), 937–944. https://doi.org/10.1016/j.soilbio.2004.09.014

Alonso, C., & Pernthaler, J. (2005). Incorporation of glucose under anoxic conditions by bacterioplankton from coastal North Sea surface waters. *Applied and Environmental Microbiology*, *71*, 1709–1716. https://doi.org/10.1128/AEM.71.4.1709-1716.2005

Anderson, T. R., & Ryabchenko, V. A. (2009). Carbon cycling in the Mesopelagic Zone of the central Arabian Sea: Results from a simple model. *Washington DC American Geophysical Union Geophysical Monograph*, *185*, 281–297. https://doi.org/10.1029/2007GM000686

Anderson, T. R., & Tang, K. W. (2010). Carbon cycling and POC turnover in the mesopelagic zone of the ocean: Insights from a simple model. *Deep Sea Research Part II Topical Studies in Oceanography*, *57*, 1581–1592. https://doi.org/10.1016/j.dsr2.2010.02.024

Arístegui, J., Agustí, S., Middelburg, J. J., & Duarte, C. M. (2005). Respiration in the mesopelagic and bathypelagic zones of the oceans. *Respiration in Aquatic Ecosystems*, 181,-205 https://doi.org/10.1093/acprof:oso/9780198527084.003.0010

Arístegui, J., Gasol, J. M., Duarte, C. M., & Herndld, G. J. (2009). Microbial oceanography of the dark ocean's pelagic realm. *Limnology and Oceanography*, *54*(5), 1501–1529. https://doi.org/10.4319/lo.2009.54.5.1501

Azam, F. (1998). Microbial control of oceanic carbon flux: The plot thickens. *Science*, *280*(5364), 694–696. https://doi.org/10.1126/science.280.5364.694

Azam, F., & Long, R. A. (2001). Sea snow microcosms. *Nature, 414*(495), 497–498. https://doi.org/10.1038/35107174

Azam, F., & Malfatti, F. (2007). Microbial structuring of marine ecosystems. *Nature Reviews Microbiology*, *5*, 782–791. https://doi.org/10.1038/nrmicro1747

Belcher, A., Iversen, M., Manno, C., Henson, S. A., Tarling, G. A., & Sanders, R. (2016). The role of particle associated microbes in remineralization of fecal pellets in the upper mesopelagic of the Scotia Sea, Antarctica. *Limnology and Oceanography*, *61*, 1049–1064. https://doi.org/10.1002/lno.10269

Berges, J. A., Franklin, D. J., & Harrison, P. J. (2001). Evolution of an artificial seawater medium: Improvements in enriched seawater, artificial water over the last two decades. *Journal of Phycology*, *37*, 1138–1145. https://doi.org/10.1046/j.1529-8817.2001.01052.x

Bidle, K. D., & Azam, F. (2001). Bacterial control of silicon regeneration from diatom detritus: Significance of bacterial ectohydrolases and species identity. *Limnology and Oceanography*, *46*(7), 1606–1623. https://doi.org/10.4319/lo.2001.46.7.1606

Boeuf, D., Edwards, B. R., Eppley, J. M., Hu, S. K., Poff, K. E., Romano, A. E., … DeLong, E. F. (2019). Biological composition and microbial dynamics of sinking particulate organic matter at abyssal depths in the oligotrophic open ocean. *Proceedings of the National Academy of Sciences*, *116*(24), 11824–11832. https://doi.org/10.1073/pnas.1903080116

Boyd, P. W., & Trull, T. W. (2007). Understanding the export of biogenic particles in oceanic waters: Is there consensus? *Progress in Oceanography*, *72*(4), 276–312. https://doi.org/10.1016/j.pocean.2006.10.007

Bubendorfer, S., Held, S., Windel, N., Paulick, A., Klingl, A., & Thormann, K. M. (2012). Specificity of motor components in the dual flagellar system of Shewanella putrefaciens CN-32. *Molecular microbiology*, *83*(2), 335–350. https://doi.org/10.1111/j.1365-2958.2011.07934.x

Buchan, A., LeCleir, G. R., Gulvik, C. A., & González, J. M. (2014). Master recyclers: Features and functions of bacteria associated with phytoplankton blooms. *Nature Reviews Microbiology*, *12*(10), 686–698. https://doi.org/10.1038/nrmicro3326

Burd, A. B., & Jackson, G. A. (2009). Particle aggregation. *Annual Review of Marine Science*, *1*, 65–90. https://doi.org/10.1146/annurev.marine.010908.163904

Caporaso, J. G., Kuczynski, J., Stombaugh, J., Bittinger, K., Bushman, F. D., Costello, E. K., … Knight, R. (2010). QIIME allows analysis of high-throughput community sequencing data. *Nature Methods*, *7*, 335–336. https://doi.org/10.1038/nmeth.f.303

Chen, X.-L., Zhang, Y.-Z., Gao, P.-J., & Luan, X.-W. (2003). Two different proteases produced by a deep-sea psychrotrophic bacterial strain, *Pseudoaltermonas* sp. SM9913. *Marine Biology*, *143*, 989–993. https://doi.org/10.1007/s00227-003-1128-2

Cho, B. C., & Azam, F. (1988). Major role of bacteria in biogeochemical fluxes in the ocean's interior. *Nature*, *332*, 441–443. https://doi.org/10.1038/332441a0

Covert, J. S., & Moran, M. A. (2001). Molecular characterization of estuarine bacterial communities that use high-and low-molecular weight fractions of dissolved organic carbon. *Aquatic Microbial Ecology*, *25*, 127–139. https://doi.org/10.3354/ame025127

Crespo, B. G., Pommier, T., Fernández-Gómez, B., & Pedrós-Alió, C. (2013). Taxonomic composition of the particle-attached and free-living bacterial assemblages in the Northwest Mediterranean Sea analyzed by pyrosequencing of the 16S rRNA. *Microbiologyopen*, *2*(4), 541–552. https://doi.org/10.1002/mbo3.92

Dang, H., & Lovell, C. R. (2016). Microbial surface colonization and biofilm development in marine environments. *Microbiology and Molecular Biology Reviews*, *80*(1), 91–138. https://doi.org/10.1128/MMBR.00037-15

DeLong, E. F., Franks, D. G., & Alldredge, A. L. (1993). Phylogenetic diversity of aggregate-attached vs. free-living marine bacterial assemblages. *Limnology & Oceanography*, *38*, 924–934. https://doi.org/10.4319/lo.1993.38.5.0924

DeLong, E. F., Preston, C. M., Mincer, T., Rich, V., Hallam, S. J., Frigaard, N. U., … Chisholm, S. W. (2006). Community genomics among stratified microbial assemblages in the ocean's interior. *Science*, *311*(5760), 496–503. https://doi.org/10.1126/science.1120250

Duret, M. T., Lampitt, R. S., & Lam, P. (2019). Prokaryotic niche partitioning between suspended and sinking marine particles. *Environmental Microbiology Reports*, *11*(3), 386–400. https://doi.org/10.1111/1758-2229.12692

Eloe, E. A., Shulse, C. N., Fadrosh, D. W., Williamson, S. J., Allen, E. E., & Bartlett, D. H. (2011). Compositional differences in particle-associated and free-living microbial assemblages from an extreme deep-ocean environment. *Environmental Microbiology Reports*, *3*, 449. https://doi.org/10.1111/j.1758-2229.2010.00223.x

Eppley, R. W., & Peterson, B. J. (1979). Particulate organic matter flux and planktonic new production in the deep ocean. *Nature*, *282*, 677–680. https://doi.org/10.1038/282677a0

Falkowski, P. G. (1998). Biogeochemical controls and feedbacks on ocean primary production. *Science*, *281*, 200–206. https://doi.org/10.1126/science.281.5374.200

Fandino, L. B., Riemann, L., Steward, G. F., Long, R. A., & Azam, F. (2001). Variations in bacterial community structure during a dinoflagellate bloom analyzed by DGGE and 16S rDNA sequencing. *Aquatic Microbial Ecology*, *23*(2), 119–130. https://doi.org/10.3354/ame023119

Fang, J., Chan, O., Kato, C., Sato, T., Peeples, T., & Nigggemeyer, K. (2003). Phospholipid fatty acid profiles of piezophilic bacteria from the deep sea. *Lipids*, *38*(8), 885–887. https://doi.org/10.1007/s11745-003-1140-7

Fang, J., Uhle, M., Billmark, K., Bartlett, D. H., & Kato, C. (2006). Fractionation of carbon isotopes in biosynthesis of fatty acids by a piezophilic bacterium *Moritella japonica* strain DSK1. *Geochimica Et Cosmochimica Acta*, *70*, 1753–1760. https://doi.org/10.1016/j.gca.2005.12.011

Fang, J., Zhang, L., &Bazylinski, D. A. (2010). Deep-sea piezosphere and piezophiles:geomicrobiology and biogeochemistry. *Trends in microbiology*, *18*(9), 413–422.https://doi.org/10.1016/j.tim.2010.06.006

Fang, J. S., Zhang, L. I., Li, J. T., Kato, C., Tamburini, C., Zhang, Y. Z., … Wang, F. P. (2015). The POM-DOM piezophilic microorganism continuum(PDPMC)—The role of piezophilic microorganisms in the global ocean carbon cycle. *Science China Earth Sciences*, *58*, 106–115. https://doi.org/10.1007/s11430-014-4985-2

Fukami, K., Simidu, U., & Taga, N. (1981). Fluctuation of the communities of heterotrophic bacteria during the decomposition process of phytoplankton. *Journal of Experimental Marine Biology and Ecology*, *55*(2–3), 171–184. https://doi.org/10.1016/0022-0981(81)90110-6

Garrett, T. R., Bhakoo, M., & Zhang, Z. (2008). Bacterial adhesion and biofilms on surfaces. *Progress in Natural Science*, *18*(9), 1049–1056. https://doi.org/10.1016/j.pnsc.2008.04.001

Ghiglione, J. F., Conan, P., & Pujopay, M. (2009). Diversity of total and active free-living vs. particle-attached bacteria in the euphotic zone of the NW Mediterranean Sea. *Fems Microbiology Letters*, *299*, 9–21. https://doi.org/10.1111/j.1574-6968.2009.01694.x

Ghiglione, J. F., Mevel, G., Pujo-Pay, M., Mousseau, L., Lebaron, P., & Goutx, M. (2007). Diel and seasonal variations in abundance, activity, and community structure of particle-attached and free-living bacteria in NW Mediterranean Sea. *Microbial Ecology*, *54*(2), 217–231. https://doi.org/10.1007/s00248-006-9189-7

Grossart,H.P.(2010).Ecologicalconsequencesofbacterioplanktonlifestyles: Changes in concepts are needed. *Environmental Microbiology Reports*, *2*(6), 706–714. https://doi.org/10.1111/j.1758-2229.2010.00179.x

Grossart, H. P., & Gust, G. (2009). Hydrostatic pressure affects physiology and community structure of marine bacteria during settling to 4000 m: an experimental approach. *Marine Ecology Progress Series*, *390*, 97–104. https://doi.org/10.3354/meps08201

Grossart, H. P., Levold, F., Allgaier, M., Simon, M., & Brinkhoff, T. (2005). Marine diatom species harbour distinct bacterial communities. *Environmental Microbiology*, *7*(6), 860–873. https://doi.org/10.1111/j.1462-2920.2005.00759.x

Grossart, H.-P., & Ploug, H. (2001). Microbial degradation of organic carbon and nitrogen on diatom aggregates. *Limnology and Oceanography*, *46*, 267–277. https://doi.org/10.4319/lo.2001.46.2.0267

Grossart, H. P., Tang, K. W., Kiørboe, T., & Ploug, H. (2007). Comparison of cell-specific activity between free-living and attached bacteria using isolates and natural assemblages. *FEMS Microbiology Letters*, *266*(2), 194–200. https://doi.org/10.1111/j.1574-6968.2006.00520.x

Guillard, R.R.L. (1975). Culture of phytoplankton for feeding marine invertebrates. In: W.L. Smith,M.H. Chanley (Eds)., *Culture of marine invertebrate animals* (pp. 29-60). Boston, MA: Springer. https://doi.org/10.1007/978-1-4615-8714-9_3

Hedges, J. I. (1992). Global biogeochemical cycles: Progress and problems. *Marine Chemistry*, *39*, 67–93. https://doi.org/10.1016/0304-4203(92)90096-S

Herndl, G. J., & Reinthaler, T. (2013). Microbial control of the dark end of the biological pump. *Nature Geoscience*, *6*(9), 718. https://doi.org/10.1038/ngeo1921

Hollibaugh, J. T., Wong, P. S., & Murrell, M. C. (2000). Similarity of particle-associated and free-living bacterial communities in northern San Francisco Bay, California. *Aquatic Microbial Ecology*, *21*(2), 103–114. https://doi.org/10.3354/ame021103

Jia, Z., & Conrad, R. (2009). Bacteria rather than archaea dominate microbial ammonia oxidation in an agricultural soil. *Environmental Microbiology*, *11*, 1658–1671. https://doi.org/10.1111/j.1462-2920.2009.01891.x

Karl, D. M., Knauer, G. A., & Martin, J. H. (1988). Downward flux of particulate organic matter in the ocean: A particle decomposition paradox. *Nature*, *332*, 438–441. https://doi.org/10.1038/332438a0

Kato, C., Sato, T., & Horikoshi, K. (1995). Isolation and properties of barophilic and barotolerant bacteria from deep-sea mud samples. *Biodiversity & Conservation*, *4*(1), 1–9. https://doi.org/10.1007/BF00115311

Kiørboe, T., Grossart, H. P., Ploug, H., & Tang, K. (2002). Mechanisms and rates of bacterial colonization of sinking aggregates. *Applied and Environment Microbiology*, *68*(8), 3996–4006. https://doi.org/10.1128/AEM.68.8.3996-4006.2002

Kiørboe, T., & Jackson, G. A. (2001). Marine snow, organic solute plumes, and optimal chemosensory behavior of bacteria. *Limnology & Oceanography*, *46*, 1309–1318. https://doi.org/10.4319/lo.2001.46.6.1309

Kumar, S., Stecher, G., & Tamura, K. (2016). MEGA7: Molecular evolutionary genetics analysis version 7.0 for bigger datasets. *Molecular Biology and Evolution*, *33*(7), 1870–1874. https://doi.org/10.1093/molbev/msw054

Lane, D. J. (1991). 16S/23S rRNA sequencing. In E. Stackebrandt & M. Goodfellow (Ed.), *Nucleic acid techniques in bacterial systematics* (pp. 115-175). New York, NY: John Wiley & Sons.

Lapoussière, A., Michel, C., Starr, M., Gosselin, M., & Poulin, M. (2011). Role of free-living and particle-attached bacteria in the recycling and export of organic material in the Hudson Bay system. *Journal of Marine Systems*, *88*, 434–445. https://doi.org/10.1016/j.jmarsys.2010.12.003

Lauro, F. M., & Bartlett, D. H. (2008). Prokaryotic lifestyles in deep sea habitats. *Extremophiles*, *12*(1), 15–25. https://doi.org/10.1007/s00792-006-0059-5

Lauro, F. M., McDougald, D., Thomas, T., Williams, T. J., Egan, S., Rice, S., … Cavicchioli, R. (2009). The genomic basis of trophic strategy in marine bacteria. *Proceedings of the National Academy of Sciences of the United States of America*, *106*(37), 15527–15533. https://doi.org/10.1073/pnas.0903507106

Lee, S. H., & Fuhrman, J. A. (1991). Species composition shift of confined bacterioplankton studied at the level of community dna. *Marine Ecology Progress Series*, *79*, 195–201. https://doi.org/10.3354/meps079195

Li, J., Wei, B., Wang, J., Liu, Y., Dasgupta, S., Zhang, L. I., & Fang, J. (2015). Variation in abundance and community structure of particle-attached and free-living bacteria in the South China Sea. *Deep Sea Research Part II Topical Studies in Oceanography*, *122*, 64–73. https://doi.org/10.1016/j.dsr2.2015.07.006

Lima, I. D., Lam, P. J., & Doney, S. C. (2014). Dynamics of particulate organic carbon flux in a global ocean model. *Biogeosciences Discussions*, *10*, 14715–14767. https://doi.org/10.5194/bgd-10-14715-2013

Liu, Q., Fang, J., Li, J., Zhang, L., Xie, B. B., Chen, X. L., & Zhang, Y. Z. (2018). Depth-resolved variations of cultivable bacteria and their extracellular enzymes in the water column of the New Britain Trench. *Frontiers in Microbiology*, *9*, 135. https://doi.org/10.3389/fmicb.2018.00135

Liu, R., Wang, L. I., Liu, Q., Wang, Z., Li, Z., Fang, J., … Luo, M. (2018). Depth-resolved distribution of particle-attached and free-living bacterial communities in the water column of the New Britain Trench. *Frontiers in Microbiology*, *9*, 625. https://doi.org/10.3389/fmicb.2018.00625

Liu, S., Wawrik, B., & Liu, Z. (2017). Different bacterial communities involved in peptide decomposition between normoxic and

hypoxic coastal waters. *Frontiers in Microbiology*, 8, 353. https://doi.org/10.3389/fmicb.2017.00353

Lueders, T., Manefield, M., & Friedrich, M. W. (2004). Enhanced sensitivity of DNA-and rRNA-based stable isotope probing by fractionation and quantitative analysis of isopycnic centrifugation gradients. *Environmental Microbiology*, 6(1), 73–78. https://doi.org/10.1046/j.1462-2920.2003.00536.x

Marietou, A., & Bartlett, D. H. (2014). Effects of high hydrostatic pressure on coastal bacterial community abundance and diversity. *Applied and Environment Microbiology*, 80(19), 5992–6003. https://doi.org/10.1128/AEM.02109-14

Martin, M., Barbeyron, T., Martin, R., Portetelle, D., Michel, G., & Vandenbol, M. (2015). The cultivable surface microbiota of the brown alga *Ascophyllum nodosum* is enriched in macroalgal-polysaccharide-degrading bacteria. *Frontiers in Microbiology*, 6, 1487. https://doi.org/10.3389/fmicb.2015.01487

Mayali, X., Stewart, B., Mabery, S., & Weber, P. K. (2016). Temporal succession in carbon incorporation from macromolecules by particle-attached bacteria in marine microcosms. *Environmental Microbiology Reports*, 8(1), 68. https://doi.org/10.1111/1758-2229.12352

Mestre, M., Ruiz-González, C., Logares, R., Duarte, C. M., Gasol, J. M., & Sala, M. M. (2018). Sinking particles promote vertical connectivity in the ocean microbiome. *Proceedings of the National Academy of Sciences*, 115(29), E6799–E6807. https://doi.org/10.1073/pnas.1802470115

Middelboe, M., & Lundsgaard, C. (2003). Microbial activity in the Greenland Sea: Role of DOC lability, mineral nutrients and temperature. *Aquatic Microbial Ecology*, 32(2), 151–163. https://doi.org/10.3354/ame032151

Moeseneder, M. M., Winter, C., & Herndl, G. J. (2001). Horizontal and vertical complexity of attached and free-living bacteria of the eastern Mediterranean Sea, determined by 16S rDNA and 16S rRNA fingerprints. *Limnology and Oceanography*, 46(1), 95–107. https://doi.org/10.3354/ame032151

Nadkarni, M. A., Martin, F. E., Jacques, N. A., & Hunter, N. (2002). Determination of bacterial load by real-time PCR using a broad-range (universal) probe and primers set. *Microbiology*, 148, 257–266. https://doi.org/10.1099/00221287-148-1-257

Nelson, C. E., & Carlson, C. A. (2012). Tracking differential incorporation of dissolved organic carbon types among diverse lineages of Sargasso Sea bacterioplankton. *Environmental Microbiology*, 14, 1500–1516. https://doi.org/10.1111/j.1462-2920.2012.02738.x

Neufeld, J. D., Dumont, M. G., Vohra, J., & Murrell, J. C. (2007). Methodological considerations for the use of stable isotope probing in microbial ecology. *Microbial Ecology*, 53, 435–442. https://doi.org/10.1007/s00248-006-9125-x

Neufeld, J. D., Vohra, J., Dumont, M. G., Lueders, T., Manefield, M., Friedrich, M. W., & Murrell, J. C. (2007). DNA stable-isotope probing. *Nature Protocols*, 2, 860–866. https://doi.org/10.1038/nprot.2007.109

Neufeld, J. D., Wagner, M., & Murrell, J. C. (2007). Who eats what, where and when? Isotope-labelling experiments are coming of age. *ISME Journal*, 1, 103–110. https://doi.org/10.1038/ismej.2007.30

Orsi, W. D., Smith, J. M., Liu, S., Liu, Z., Sakamoto, C. M., Wilken, S., ... Santoro, A. E. (2016). Diverse, uncultivated bacteria and archaea underlying the cycling of dissolved protein in the ocean. *The ISME Journal*, 10(9), 2158. https://doi.org/10.1038/ismej.2016.20

Pande, S., Kaftan, F., Lang, S., Svatoš, A., Germerodt, S., & Kost, C. (2016). Privatization of cooperative benefits stabilizes mutualistic cross-feeding interactions in spatially structured environments. *ISME Journal*, 10(6), 1413. https://doi.org/10.1038/ismej.2015.212

Pasotti, F., Troch, M. D., Raes, M., & Vanreusel, A. (2012). Feeding ecology of shallow water meiofauna: Insights from a stable isotope tracer experiment in Potter Cove, King George Island, *Antarctica*. *Polar Biology*, 35, 1629–1640. https://doi.org/10.1007/s00300-012-1203-6

Peoples, L. M., Donaldson, S., Osuntokun, O., Xia, Q., Nelson, A., Blanton, J., ... Bartlett, D. H. (2018). Vertically distinct microbial communities in the Mariana and Kermadec trenches. *PLoS ONE*, 13(4), e0195102. https://doi.org/10.1371/journal.pone.0195102

Pinheiro, J., Bates,D., DebRoy, S., & Sarkar, D.the R Development Core Team. 2012. nlme: Linear and nonlinear mixed effects models. R package v. 3.1–104. Vienna, Austria: R Found. Stat. Comput.

Pomeroy, L. R., & Wiebe, W. J. (2001). Temperature and substrates as interactive limiting factors for marine heterotrophic bacteria. *Aquatic Microbial Ecology*, 23(2), 187–204. https://doi.org/10.3354/ame023187

Qin, Q.-L., Li, Y., Zhang, Y.-J., Zhou, Z.-M., Zhang, W.-X., Chen, X.-L., ... Zhang, Y.-Z. (2011). Comparative genomics reveals a deep-sea sediment-adapted life style of *Pseudoalteromonas* sp. SM9913. *The ISME Journal*, 5, 274. https://doi.org/10.1038/ismej.2010.103

Radajewski, S., Ineson, P., Parekh, N. R., & Murrell, J. C. (2000). Stable-isotope probing as a tool in microbial ecology. *Nature*, 403, 646–649. https://doi.org/10.1038/35001054

Radajewski, S., Mcdonald, I. R., & Murrell, J. C. (2003). Stable-isotope probing of nucleic acids: A window to the function of uncultured microorganisms. *Current Opinion in Biotechnology*, 14(3), 296–302. https://doi.org/10.1016/S0958-1669(03)00064-8

Reisch, C. R., Crabb, W. M., Gifford, S. M., Teng, Q., Stoudemayer, M. J., Moran, M. A., & Whitman, W. B. (2013). Metabolism of dimethylsulphoniopropionate by *Ruegeria pomeroyi* DSS-3. *Molecular Microbiology*, 89(4), 774–791. https://doi.org/10.1111/mmi.12314

Reisch, C. R., Moran, M. A., & Whitman, W. B. (2011). Bacterial catabolism of dimethylsulfoniopropionate (DMSP). *Frontiers in Microbiology*, 2, 172. https://doi.org/10.3389/fmicb.2011.00172

Riemann, L., & Winding, A. (2001). Community dynamics of free-living and particle-associated bacterial assemblages during a freshwater phytoplankton bloom. *Microbial Ecology*, 42(3), 274–285. https://doi.org/10.1007/s00248-001-0018-8

Salazar, G., Cornejo-Castillo, F. M., Benítez-Barrios, V., Fraile-Nuez, E., Álvarez-Salgado, X. A., Duarte, C. M., ... Acinas, S. G. (2016). Global diversity and biogeography of deep-sea pelagic prokaryotes. *The ISME Journal*, 10(3), 596. https://doi.org/10.1038/ismej.2015.137

Seth, E. C., & Taga, M. E. (2014). Nutrient cross-feeding in the microbial world. *Frontiers in Microbiology*, 5(350), 350. https://doi.org/10.3389/fmicb.2014.00350

Simon, M., Grossart, H.-P., Schweitzer, B., & Ploug, H. (2002). Microbial ecology of organic aggregates in aquatic ecosystems. *Aquatic Microbial Ecology*, 28, 175–211. https://doi.org/10.3354/ame028175

Smith, D. C., Simon, M., Alldredge, A. L., & Azam, F. (1992). Intense hydrolytic enzyme activity on marine aggregates and implications for rapid particle dissolution. *Nature*, 359, 139–142. https://doi.org/10.1038/359139a0

Sogin, M. L., Morrison, H. G., Huber, J. A., Welch, D. M., Huse, S. M., Neal, P. R., ... Herndl, G. J. (2006). Microbial diversity in the deep sea and the underexplored "rare biosphere". *Proceedings of the National Academy of Sciences of the United States of America*, 103, 12115–12120. https://doi.org/10.1073/pnas.0605127103

Steinberg, D. K., Mooy, B. A. S. V., Buesseler, K. O., Boyd, P. W., Kobari, T., & Karl, D. M. (2008). Bacterial vs. zooplankton control of sinking particle flux in the ocean's twilight zone. *Limnology & Oceanography*, 53, 1327–1338. https://doi.org/10.4319/lo.2008.53.4.1327

Stubner, S. (2002). Enumeration of 16S rDNA of Desulfotomaculum lineage 1 in rice field soil by real-time PCR with SybrGreen™ detection. *Journal of Microbiological Methods*, 50, 155–164. https://doi.org/10.1016/S0167-7012(02)00024-6

Suroy, M., Panagiotopoulos, C., Boutorh, J., Goutx, M., & Moriceau, B. (2015). Degradation of diatom carbohydrates: A case study with N-and Si-stressed *Thalassiosira weissflogii*. *Journal of Experimental Marine Biology and Ecology*, 470, 1–11. https://doi.org/10.1016/j.jembe.2015.04.018

Tamburini, C., Boutrif, M., Garel, M., Colwell, R. R., & Deming, J. W. (2013). Prokaryotic responses to hydrostatic pressure in the ocean–a review. _Environmental Microbiology_, _15_(5), 1262–1274. https://doi.org/10.1111/1462-2920.12084

Tamburini, C., Garcin, J., Grégori, G., Leblanc, K., Rimmelin, P., & Kirchman, D. L. (2006). Pressure effects on surface Mediterranean prokaryotes and biogenic silica dissolution during a diatom sinking experiment. _Aquatic Microbial Ecology_, _43_(3), 267–276. https://doi.org/10.3354/ame043267

Tamburini, C., Garcin, J., Ragot, M., & Bianchi, A. (2002). Biopolymer hydrolysis and bacterial production under ambient hydrostatic pressure through a 2000 m water column in the NW Mediterranean. _Deep Sea Research Part II: Topical Studies in Oceanography_, _49_(11), 2109–2123. https://doi.org/10.1016/S0967-0645(02)00030-9

Tamburini, C., Garcin, J., & Bianchi, A. (2003). Role of deep-sea bacteria in organic matter mineralization and adaptation to hydrostatic pressure conditions in the NW Mediterranean Sea. _Aquatic Microbial Ecology_, _32_(3), 209–218. https://doi.org/10.3354/ame032209

Tamburini, C., Goutx, M., Guigue, C., Garel, M., Lefèvre, D., Charrière, B., … Lee, C. (2009). Effects of hydrostatic pressure on microbial alteration of sinking fecal pellets. _Deep Sea Research Part II: Topical Studies in Oceanography_, _56_(18), 1533–1546. https://doi.org/10.1016/j.dsr2.2008.12.035

Teeling, H., Fuchs, B. M., Becher, D., Klockow, C., Gardebrecht, A., Bennke, C. M., … Amann, R. (2012). Substrate-controlled succession of marine bacterioplankton populations induced by a phytoplankton bloom. _Science_, _336_(6081), 608–611. https://doi.org/10.1126/science.1218344

Thiele, S., Fuchs, B. M., Amann, R., & Iversen, M. H. (2015). Colonization in the photic zone and subsequent changes during sinking determine bacterial community composition in marine snow. _Applied and Environment Microbiology_, _81_(4), 1463–1471. https://doi.org/10.1128/AEM.02570-14

Turley, C. M. (1993). The effect of pressure on leucine and thymidine incorporation by free-living bacteria and by bacteria attached to sinking oceanic particles. _Deep Sea Research Part I: Oceanographic Research Papers_, _40_(11–12), 2193–2206. https://doi.org/10.1016/0967-0637(93)90098-N

Turner, J. T. (2015). Zooplankton fecal pellets, marine snow, phytodetritus and the ocean's biological pump. _Progress in Oceanography_, _130_, 205–248. https://doi.org/10.1016/j.pocean.2014.08.005

Verdugo, P., Alldredge, A. L., Azam, F., Kirchman, D. L., Passow, U., & Santschi, P. H. (2004). The oceanic gel phase: A bridge in the DOM–POM continuum. _Marine Chemistry_, _92_(1–4), 67–85. https://doi.org/10.1016/j.marchem.2004.06.017

Volk T, Hoffert M I. 1985. Ocean carbon pumps: Analysis of relative strengths and efficiencies in ocean-driven atmospheric CO2 changes. In: E T Sundquist, W S Broecker Eds., _The Carbon Cycle and Atmospheric CO2: Natural Variations Archean to Present_. (pp 99–110.Washington DC: American Geophysical Union. https://doi.org/10.1029/GM032p0099

Wakeham, S. G., & Lee, C. (1993). Production, transport, and alteration of particulate organic matter in the marine water column. In: M.H. Engel, S.A. Macko (Eds)., _Organic geochemistry .Topics in Geobiology_, _11_,(pp. 145-169). Boston, MA: Springerhttps://xs.scihub.ltd/https://doi.org/10.1007/978-1-4615-2890-6_6

Wang, X., Sharp, C. E., Jones, G. M., Grasby, S. E., Brady, A. L., & Dunfield, P. F. (2015). Stable-isotope-probing identifies uncultured planctomycetes as primary degraders of a complex heteropolysaccharide in soil. _Applied and Environmental Microbiology_, _81_(14), 4607. https://doi.org/10.1128/AEM.00055-15

Wilson, S. E., Steinberg, D. K., & Buesseler, K. O. (2008). Changes in fecal pellet characteristics with depth as indicators of zooplankton repackaging of particles in the mesopelagic zone of the subtropical and subarctic North Pacific Ocean. _Deep-Sea Research Part II_, _55_, 1636–1647. https://doi.org/10.1016/j.dsr2.2008.04.019

APPENDIX
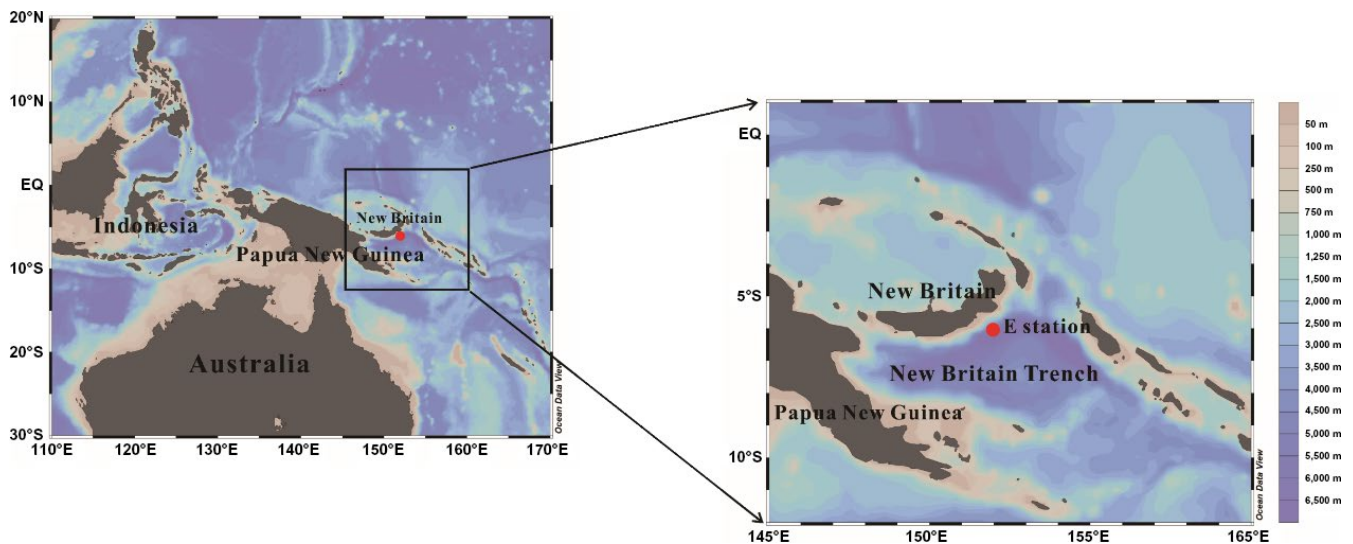
FIGURE A1 Locations of the seawater sampling sites in the New Britain Trench (E station)
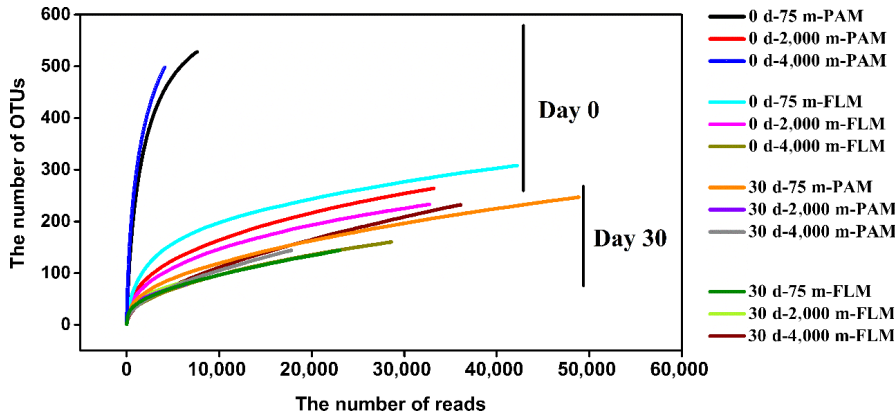
FIGURE A2 Rarefaction curves of the PAM and FLM at 0.1, 20, and 40 MPa and 15°C at day 0 and day 30 at a cutoff value of 97% sequence similarity
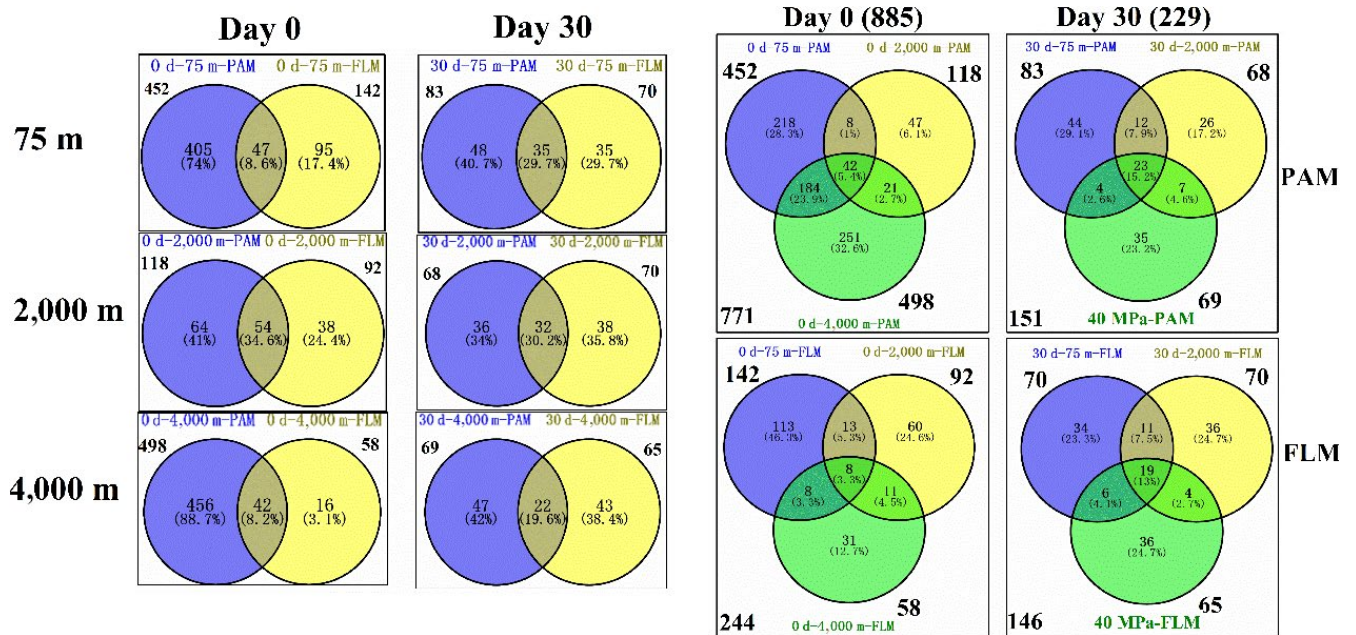
FIGURE A3 Venn diagrams showing changes in shared and unique total OTUs between the PAM and FLM assemblages incubated at 0.1, 20, and 40 MPa and 15°C at day 0 and day 30
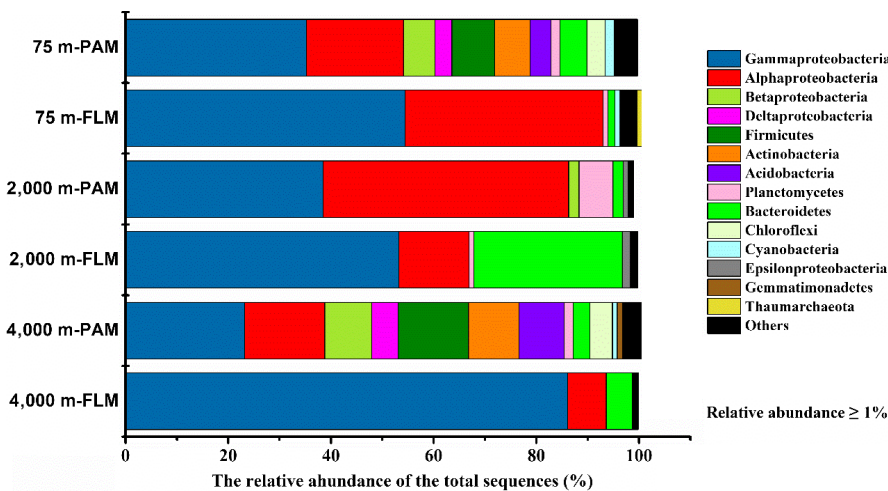
FIGURE A4 The relative abundance of the most abundant phylum (class) (≥1%) in PAM and FLM communities at 75, 2,000, and 4,000 m three depths in the NBT at day 0
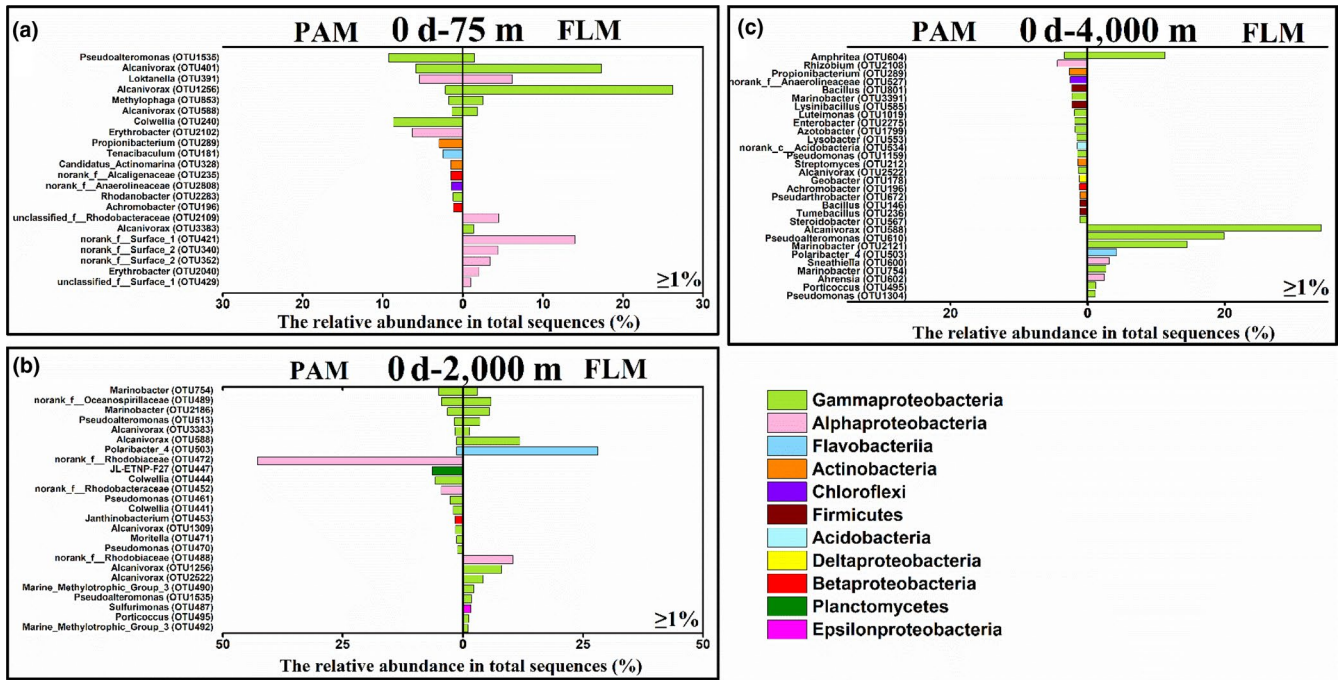
FIGURE A5 The relative abundance of the most abundant genera (OTUs) (≥1%) in PAM and FLM communities at 75 (a), 2,000 (b), and 4,000 m (c) in the NBT at day 0
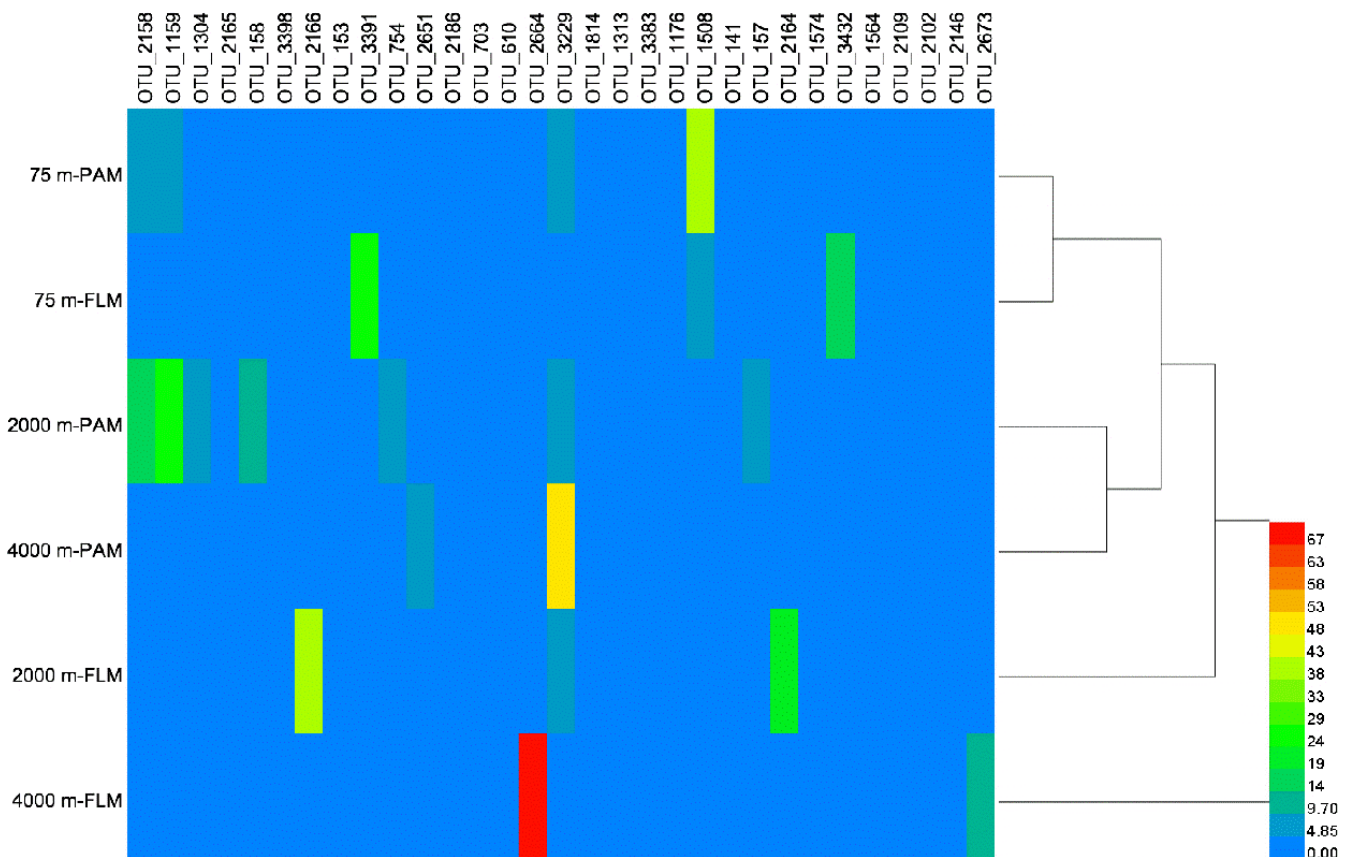
FIGURE A6 Hierarchically clustered heatmap of the representive OTUs in PAM and FLM for POC decomposition at 0.1, 20, and 40 MPa under 15°C after 30-day incubation

TABLE A1 The physical and chemical parameters in the water column of the New Britain Trench

Depth (m)	Temperature (°C)	Salinity (PSU)	Oxygen (mg/L)	POC (mg/L)	Bacterial abundance (cells/ml)
75	27.2	35.1	5.6	0.02	1×10^5
2,000	2.3	34.6	3.8	0.02	1×10^4
4,000	2.0	34.7	4.7	0.01	1×10^4

TABLE A2 POC and DOC concentrations, and POC degradation rates for the ^{13}C-labeled and ^{12}C-control treatments in PAM and FLM incubations at 0.1, 20, and 40 MPa and 15°C at day 0 and day 30

		The concentration of ^{13}C-POC				The concentration of ^{12}C-POC			
		PAM (mg/L)		FLM (mg/L)		PAM (mg/L)		FLM (mg/L)	
Pressure (MPa)	Time (day)	Mean	POC Degradation Rate (μmol C L^{-1} day^{-1})	Mean	POC Degradation Rate (μmol C L^{-1} day^{-1})	Mean	POC Degradation Rate (μmol C L^{-1} day^{-1})	Mean	POC Degradation Rate (μmol C L^{-1} day^{-1})
0.1	0	54	0.025	47.5	0.012	65.1	0.028	55.7	0.028
	30	25.7		33.5		28.4		23.9	
20	0	55.6	0.011	53.2	0.018	50.4	0.016	51.0	0.011
	30	40.4		31.3		31.5		36.5	
40	0	53.3	0.009	71.2	0.021	55.4	0.006	57.3	0.030
	30	40.5		38.1		46.8		23.4	

		The concentration of ^{13}C-DOC		The concentration of ^{12}C-DOC	
Pressure (MPa)	Time (day)	PAM (mg/L)	FLM (mg/L)	PAM (mg/L)	FLM (mg/L)
0.1	0	18.3	15.0	103	81
	30	10.9	12.4	55	50
20	0	17.8	15.2	77	81
	30	29.9	28.2	161	142
40	0	16.2	18.6	78	80
	30	31.0	25.8	132	158

TABLE A3 The δ^{13}C values of POC and DOC in the PAM and FLM cultures at 0.1, 20, and 40 MPa at day 30 (a) and ^{13}C atom % that utilized by PAM and FLM (b)

(a)

		The δ^{13}C value of POC and DOC in PAM culture system at day 30				The δ^{13}C value of POC and DOC in FLM culture system at day 30			
		POC		DOC		POC		DOC	
Treatments	Depth (m)	δ^{13}C (‰)	^{13}C atom (%)	δ^{13}C (‰)	^{13}C atom (%)	δ^{13}C (‰)	^{13}C atom (%)	δ^{13}C (‰)	^{13}C atom (%)
^{13}C-labeled	75	170,437.2	67.49	125,864.8	60.58	183,508.9	69.09	124,270.8	60.27
	2,000	187,652.4	69.56	122,270.6	59.89	187,534.9	69.54	122,710.8	59.97
	4,000	196,041.6	70.47	129,673.6	61.28	175,908.1	68.18	109,681.8	57.28
^{12}C-control	75	873.8	2.22	528.3	1.82	67.1	1.28	284.8	1.53
	2,000	197.6	1.43	746.3	2.07	231.0	1.47	676.1	1.99
	4,000	392.1	1.66	652.8	1.96	115.9	1.33	623.0	1.93

(b)

		The ^{13}C atom% of DOC in PAM culture system (%)			The ^{13}C atom% of DOC in FLM culture system (%)		
Treatments	Depth (m)	Day 0	Day 30	Utilization by PAM	Day 0	Day 30	Utilization by FLM
^{13}C	75	71.7	60.58	11.1	71.7	60.27	11.4
	2,000	71.7	59.89	11.8	71.7	59.97	11.7
	4,000	71.7	61.28	10.4	71.7	57.28	14.4

TABLE A4 The 16S rRNA gene copy number of the 3th-14th DNA gradient fractions in the PAM and FLM assemblages at 0.1, 20, and 40 MPa by quantitative PCR after 30-d incubation. (a) 13C-PAM; (b) 12C-PAM; (c) 13C-FLM; and (d) 12C-FLM

(a) 13C-PAM

DNA fraction	CsCl buoyant density (g/ml)	0.1 MPa				20 MPa				40 MPa			
		1	2	3	Mean	1	2	3	Mean	1	2	3	Mean
3	1.7479	6.29E+03	6.29E+03	6.29E+03	6.29E+03	6.37E+03	6.30E+03	7.32E+03	6.66E+03	3.11E+03	3.14E+03	4.33E+03	3.53E+03
4	1.7445	5.83E+03	5.83E+03	5.83E+03	5.83E+03	3.01E+04	2.53E+04	2.76E+04	2.77E+04	1.12E+04	1.11E+04	1.13E+04	1.12E+04
5	1.7399	5.13E+05	5.13E+05	5.13E+05	5.13E+05	3.93E+05	4.21E+05	4.24E+05	4.13E+05	4.05E+05	4.08E+05	3.81E+05	3.98E+05
6	1.7365	5.15E+06	5.15E+06	5.15E+06	5.15E+06	2.04E+06	2.13E+06	2.12E+06	2.10E+06	2.39E+06	2.56E+06	2.63E+06	2.53E+06
7	1.7331	1.97E+06	1.97E+06	1.97E+06	1.97E+06	9.63E+05	9.39E+05	1.01E+06	9.72E+05	6.71E+05	6.28E+05	7.02E+05	6.67E+05
8	1.7296	6.24E+06	6.24E+06	6.24E+06	6.24E+06	7.36E+05	6.26E+05	6.60E+05	6.74E+05	2.21E+05	2.08E+05	2.15E+05	2.15E+05
9	1.7250	5.54E+05	5.54E+05	5.54E+05	5.54E+05	1.06E+05	9.70E+04	1.03E+05	1.02E+05	5.54E+04	5.76E+04	5.34E+04	5.55E+04
10	1.7216	2.55E+04	2.55E+04	2.55E+04	2.55E+04	1.02E+04	9.79E+03	8.76E+03	9.58E+03	2.79E+03	2.61E+03	2.32E+03	2.57E+03
11	1.7170	1.16E+04	1.16E+04	1.16E+04	1.16E+04	2.33E+04	2.42E+04	2.45E+04	2.40E+04	1.94E+03	1.91E+03	2.04E+03	1.96E+03
12	1.7135	1.40E+04	1.40E+04	1.40E+04	1.40E+04	2.58E+04	3.27E+04	3.16E+04	3.00E+04	3.12E+03	2.48E+03	1.28E+04	6.14E+03
13	1.7088	1.65E+03	1.65E+03	1.65E+03	1.65E+03	2.81E+03	1.80E+03	2.29E+03	2.30E+03	3.43E+02	2.42E+02	2.11E+02	2.66E+02
14	1.7065	3.26E+02	3.26E+02	3.26E+02	3.26E+02	4.59E+02	4.76E+02	5.71E+02	5.02E+02	2.88E+02	3.03E+02	3.32E+02	3.07E+02

(b) 12C-PAM

DNA fraction	CsCl buoyant density (g/ml)	0.1 MPa				20 MPa				40 MPa			
		1	2	3	Mean	1	2	3	Mean	1	2	3	Mean
3	1.7479	2.98E+02	2.98E+02	2.98E+02	2.98E+02	3.61E+03	3.75E+03	4.57E+03	3.98E+03	3.31E+02	4.14E+02	4.85E+02	4.10E+02
4	1.7445	1.83E+03	1.83E+03	1.83E+03	1.83E+03	5.44E+03	5.38E+03	4.90E+03	5.24E+03	2.20E+03	2.05E+03	2.19E+03	2.15E+03
5	1.7399	8.72E+02	8.72E+02	8.72E+02	8.72E+02	8.36E+03	6.90E+03	8.06E+03	7.77E+03	2.83E+03	2.57E+03	2.55E+03	2.65E+03
6	1.7365	7.41E+02	7.41E+02	7.41E+02	7.41E+02	1.19E+04	1.09E+04	1.06E+04	1.11E+04	3.13E+03	2.91E+03	2.25E+03	2.76E+03
7	1.7331	6.09E+03	6.09E+03	6.09E+03	6.09E+03	2.83E+04	2.81E+04	2.56E+04	2.73E+04	2.88E+03	2.78E+03	5.00E+04	1.86E+04
8	1.7296	7.98E+03	7.98E+03	7.98E+03	7.98E+03	1.90E+05	1.93E+05	2.08E+05	1.97E+05	7.49E+03	8.01E+03	8.46E+03	7.99E+03
9	1.7250	1.28E+05	1.28E+05	1.28E+05	1.28E+05	1.96E+06	1.79E+06	1.68E+06	1.81E+06	1.02E+05	7.95E+04	7.64E+04	8.58E+04
10	1.7216	2.58E+06	2.58E+06	2.58E+06	2.58E+06	4.67E+06	4.55E+06	4.41E+06	4.55E+06	5.67E+05	5.73E+05	5.94E+05	5.78E+05
11	1.7170	4.64E+06	4.64E+06	4.64E+06	4.64E+06	2.22E+06	2.38E+06	2.55E+06	2.38E+06	3.14E+05	3.30E+05	3.22E+05	3.22E+05
12	1.7135	9.24E+05	9.24E+05	9.24E+05	9.24E+05	4.13E+06	4.22E+06	3.54E+06	3.96E+06	4.33E+04	3.95E+04	3.92E+04	4.07E+04
13	1.7088	3.60E+05	3.60E+05	3.60E+05	3.60E+05	2.18E+05	2.07E+05	2.17E+05	2.14E+05	7.85E+03	8.23E+03	5.43E+03	7.17E+03
14	1.7065	4.32E+03	4.32E+03	4.32E+03	4.32E+03	2.31E+03	2.67E+03	2.33E+03	2.44E+03	4.11E+02	4.45E+02	4.13E+02	4.23E+02

(Continues)

TABLE A4 (Continued)

(c)

^{13}C-FLM

DNA fraction	CsCl buoyant density (g/ml)	0.1 MPa				20 MPa				40 MPa			
		1	2	3	Mean	1	2	3	Mean	1	2	3	Mean
3	1.7479	4.39E+02	4.88E+02	4.57E+02	4.61E+02	1.58E+03	1.79E+03	1.77E+03	1.71E+03	1.49E+03	1.72E+03	1.66E+03	1.62E+03
4	1.7445	4.96E+03	5.05E+03	5.29E+03	5.10E+03	3.53E+03	3.07E+03	3.76E+03	3.45E+03	3.40E+03	3.71E+03	3.27E+03	3.46E+03
5	1.7399	5.30E+05	5.83E+05	5.83E+05	5.65E+05	7.21E+05	8.40E+05	8.19E+05	7.93E+05	2.37E+04	2.40E+04	2.43E+04	2.40E+04
6	1.7365	2.44E+06	2.53E+06	2.74E+06	2.57E+06	5.02E+06	5.31E+06	5.10E+06	5.14E+06	2.03E+05	1.77E+05	1.87E+05	1.89E+05
7	1.7331	5.40E+05	5.53E+05	5.19E+05	5.37E+05	1.10E+06	9.51E+05	1.06E+06	1.04E+06	2.60E+05	2.36E+05	2.28E+05	2.41E+05
8	1.7296	4.04E+05	3.56E+05	3.51E+05	3.71E+05	3.82E+06	3.55E+06	3.70E+06	3.69E+06	3.34E+05	3.23E+05	3.18E+05	3.25E+05
9	1.7250	3.79E+04	2.38E+04	3.56E+04	3.25E+04	1.42E+06	1.56E+06	1.35E+06	1.44E+06	7.18E+04	8.54E+04	8.52E+04	8.08E+04
10	1.7216	5.30E+03	5.54E+03	5.60E+03	5.48E+03	1.50E+05	1.58E+05	1.46E+05	1.52E+05	2.64E+03	2.57E+03	2.34E+03	2.52E+03
11	1.7170	7.03E+03	6.31E+03	6.77E+03	6.70E+03	7.33E+04	7.18E+04	6.91E+04	7.14E+04	1.93E+03	1.92E+03	1.87E+03	1.91E+03
12	1.7135	2.90E+03	3.00E+03	2.77E+03	2.89E+03	3.57E+04	3.29E+04	3.00E+04	3.29E+04	2.70E+03	2.53E+03	2.57E+03	2.60E+03
13	1.7088	6.64E+01	8.49E+01	1.15E+02	8.88E+01	3.30E+03	3.03E+03	3.15E+03	3.16E+03	2.19E+02	1.50E+02	2.03E+02	1.91E+02
14	1.7065	2.60E+02	1.58E+02	1.74E+02	1.98E+02	1.67E+03	1.25E+03	1.24E+03	1.39E+03	1.40E+02	1.42E+02	1.11E+02	1.31E+02

(d)

^{12}C-FLM

DNA fraction	CsCl buoyant density (g/ml)	0.1 MPa				20 MPa				40 MPa			
		1	2	3	Mean	1	2	3	Mean	1	2	3	Mean
3	1.7479	3.31E+02	2.72E+02	3.06E+02	3.03E+02	1.35E+02	4.49E+01	7.16E+01	8.38E+01	7.63E+02	1.01E+03	7.02E+02	8.24E+02
4	1.7445	3.27E+02	3.19E+02	4.92E+02	3.79E+02	1.69E+02	8.32E+01	7.58E+01	1.09E+02	2.39E+02	2.15E+02	2.03E+02	2.19E+02
5	1.7399	6.92E+02	6.31E+02	7.06E+02	6.76E+02	1.30E+02	1.12E+02	1.52E+02	1.31E+02	1.18E+03	1.17E+03	1.27E+03	1.21E+03
6	1.7365	4.58E+03	4.65E+03	2.11E+04	1.01E+04	2.11E+02	1.61E+02	9.43E+01	1.56E+02	1.11E+03	8.85E+02	1.14E+03	1.05E+03
7	1.7331	8.57E+03	8.40E+03	7.75E+03	8.24E+03	1.07E+02	8.82E+01	7.61E+01	9.03E+01	2.11E+03	1.69E+03	1.64E+03	1.81E+03
8	1.7296	3.15E+04	2.94E+04	2.57E+04	2.89E+04	1.42E+02	6.37E+01	7.43E+01	9.33E+01	2.66E+03	2.53E+03	2.44E+03	2.54E+03
9	1.7250	8.83E+05	8.41E+05	7.15E+05	8.13E+05	8.14E+02	8.25E+02	6.70E+02	7.70E+02	9.85E+04	8.67E+04	9.08E+04	9.20E+04
10	1.7216	1.31E+07	1.25E+07	9.90E+06	1.19E+07	1.10E+03	9.84E+02	1.01E+03	1.03E+03	1.17E+06	1.11E+06	1.04E+06	1.11E+06
11	1.7170	4.54E+06	4.76E+06	4.12E+06	4.47E+06	1.33E+04	1.32E+04	1.25E+04	1.30E+04	3.39E+06	3.34E+06	3.42E+06	3.38E+06
12	1.7135	4.22E+06	4.58E+06	4.48E+06	4.43E+06	5.42E+03	4.81E+03	4.88E+03	5.04E+03	1.64E+06	1.41E+06	1.55E+06	1.53E+06
13	1.7088	1.58E+06	1.32E+06	1.31E+06	1.40E+06	1.66E+03	1.66E+03	1.38E+03	1.57E+03	2.77E+05	2.71E+05	2.47E+05	2.65E+05
14	1.7065	3.14E+04	2.20E+04	2.31E+04	2.55E+04	2.67E+02	2.36E+02	1.80E+02	2.28E+02	5.00E+03	4.43E+03	3.62E+03	4.35E+03

TABLE A5 The maximum number of 16S rRNA gene copies and CsCl buoyant density shift in the PAM and FLM assemblages at 0.1, 20, and 40 MPa under 15°C condition in ^{13}C-labeled and ^{12}C-control treatments after 30-d incubation

| | ^{13}C-labeled treatment | | | ^{12}C-control treatment | | | |
Sample ID	The maximum 16S rRNA gene copy number	The 16S rRNA gene copy number	CsCl buoyant density (g/ml)	The maximum 16S rRNA gene copy number	The16S rRNA gene copy number	CsCl buoyant density (g/ml)	CsCl buoyant density (BD) shift from ^{12}C-control to ^{13}C-labeled (g/ml)
30d-0.1MPa-PAM	The 6th fraction	5.15E+06	1.7365	the 11th fraction	4.64E+06	1.7170	0.020
30d-20MPa-PAM	The 6th fraction	2.10E+06	1.7365	the 10th fraction	4.55E+06	1.7216	0.015
30d-40MPa-PAM	The 6th fraction	2.53E+06	1.7365	the 10th fraction	5.78E+05	1.7216	0.015
30d-0.1MPa-FLM	The 6th fraction	2.57E+06	1.7365	the 10th fraction	1.19E+07	1.7216	0.015
30d-20MPa-FLM	The 6th fraction	5.14E+06	1.7365	the 11th fraction	1.30E+04	1.7170	0.020
30d-40MPa-FLM	The 8th fraction	3.25E+05	1.7296	the 11th fraction	3.38E+06	1.7170	0.013

TABLE A6 The α-diversity indices of the PAM and FLM assemblages at 0.1, 20, and 40 MPa under 15°C condition at day 0 and day 30 at 97% sequence similarity (All sequences had been normalized before being used for diversity analysis in this study)

Time (day)	PAM/FLM	Depth (m)	Reads	OTUs	Shannon	Simpson	Ace	Chao	Coverage (%)
0	PAM	75	4,099	452	4.65	0.03	585.65	598.99	98.6
		2,000	4,099	118	2.66	0.20	512.64	418.50	99.7
		4,000	4,099	498	5.26	0.01	620.64	598.56	96.6
	FLM	75	4,099	142	2.80	0.13	548.46	495.04	99.8
		2,000	4,099	92	2.76	0.12	433.15	345.59	99.7
		4,000	4,099	58	2.10	0.19	411.76	266.73	99.7
30	PAM	75	4,099	83	2.11	0.28	694.88	440.89	99.8
		2,000	4,099	68	2.37	0.15	174.47	120.00	99.6
		4,000	4,099	69	1.71	0.32	554.81	336.56	99.6
	FLM	75	4,099	70	2.26	0.17	517.29	346.15	99.7
		2,000	4,099	70	2.19	0.23	229.91	157.11	99.6
		4,000	4,099	65	1.19	0.55	729.83	482.80	99.6

TABLE A7 The number and relative abundance of shared and unique active OTUs between the PAM and FLM assemblages at 0.1, 20, and 40 MPa under 15°C condition after incubation

Active OTUs in three depths	The number of active OTUs	The total OTUs in day 30	The proportion of active OTUs (%)	The number of reads in active OTUs	The total reads in day 30	The relative abundance of active OTUs (%)
Only PAM	8	229	3%	6,676	228,121	3%
Only FLM	14		6%	47,886		21%
Shared PAM and FLM	9		4%	70,817		31%
SUM	31			125,379		55%

TABLE A8 The phylogenetic classification and increased relative abundance of the most active OTUs for POC decomposition at 0.1, 20, and 40 MPa under 15°C condition after incubation

Domain	Kingdom	Phylum	Classes	Orders	Family	Active Genera	Species	Active OTUs	0.1 MPa		20 MPa		40 MPa	
									PAM	FLM	PAM	FLM	PAM	FLM
Bacteria	norank	Proteobacteria	Gammaproteobacteria	Pseudomonadales	Pseudomonadaceae	Pseudomonas	unclassified_g__Pseudomonas	OTU2158	7.5	1.6	18.0	0.0	0.0	0.0
Bacteria	norank	Proteobacteria	Gammaproteobacteria	Pseudomonadales	Pseudomonadaceae	Pseudomonas	unclassified_g__Pseudomonas	OTU1159	5.2	0.0	26.6	0.0	0.0	0.0
Bacteria	norank	Proteobacteria	Gammaproteobacteria	Pseudomonadales	Pseudomonadaceae	Pseudomonas	Pseudomonas_pachastrellae	OTU1304	1.0	0.0	5.8	2.8	0.0	0.0
Bacteria	norank	Proteobacteria	Gammaproteobacteria	Pseudomonadales	Pseudomonadaceae	Pseudomonas	unclassified_g__Pseudomonas	OTU2165	1.0	0.0	0.0	2.2	0.0	0.0
Bacteria	norank	Proteobacteria	Gammaproteobacteria	Pseudomonadales	Pseudomonadaceae	Pseudomonas	unclassified_g__Pseudomonas	OTU158	0.0	0.0	11.2	0.0	0.0	0.0
Bacteria	norank	Proteobacteria	Gammaproteobacteria	Pseudomonadales	Pseudomonadaceae	Pseudomonas	unclassified_g__Pseudomonas	OTU3398	0.0	0.0	1.2	0.0	0.0	0.0
Bacteria	norank	Proteobacteria	Gammaproteobacteria	Pseudomonadales	Pseudomonadaceae	Pseudomonas	unclassified_g__Pseudomonas	OTU2166	0.0	0.0	0.0	41.7	0.0	0.0
Bacteria	norank	Proteobacteria	Gammaproteobacteria	Pseudomonadales	Pseudomonadaceae	Pseudomonas	unclassified_g__Pseudomonas	OTU153	0.0	0.0	0.0	2.4	0.0	0.0
Bacteria	norank	Proteobacteria	Gammaproteobacteria	Alteromonadales	Alteromonadaceae	Marinobacter	unclassified_g__Marinobacter	OTU3391	3.0	25.1	1.3	0.0	0.0	0.0
Bacteria	norank	Proteobacteria	Gammaproteobacteria	Alteromonadales	Alteromonadaceae	Marinobacter	Marinobacter_sediminum	OTU754	1.4	0.0	7.9	2.9	0.0	0.0
Bacteria	norank	Proteobacteria	Gammaproteobacteria	Alteromonadales	Alteromonadaceae	Marinobacter	Marinobacter_adhaerens_HP15	OTU2651	0.0	3.0	0.0	0.0	5.1	0.0
Bacteria	norank	Proteobacteria	Gammaproteobacteria	Alteromonadales	Alteromonadaceae	Marinobacter	Marinobacter_algicola	OTU2186	0.0	0.0	0.0	1.9	0.0	0.0
Bacteria	norank	Proteobacteria	Gammaproteobacteria	Alteromonadales	Alteromonadaceae	Alteromonas	unclassified_g__Alteromonas	OTU703	0.0	0.0	1.2	0.0	0.0	0.0
Bacteria	norank	Proteobacteria	Gammaproteobacteria	Alteromonadales	Pseudoalteromonadaceae	Pseudoalteromonas	Pseudoalteromonas_shioyasakiensis	OTU610	0.0	0.0	1.8	0.0	0.0	4.0
Bacteria	norank	Proteobacteria	Gammaproteobacteria	Alteromonadales	Pseudoalteromonadaceae	Pseudoalteromonas	unclassified_g__Pseudoalteromonas	OTU2664	0.0	0.0	0.0	0.0	0.0	72.8
Bacteria	norank	Proteobacteria	Gammaproteobacteria	Oceanospirillales	Halomonadaceae	Halomonas	unclassified_g__Halomonas	OTU3229	7.4	0.0	6.5	4.9	48.4	0.0
Bacteria	norank	Proteobacteria	Gammaproteobacteria	Oceanospirillales	Halomonadaceae	Halomonas	unclassified_g__Halomonas	OTU1814	0.0	0.0	0.0	0.0	1.5	0.0
Bacteria	norank	Proteobacteria	Gammaproteobacteria	Oceanospirillales	Halomonadaceae	Halomonas	unclassified_g__Halomonas	OTU1313	0.0	0.0	0.0	0.0	2.9	0.0
Bacteria	norank	Proteobacteria	Gammaproteobacteria	Oceanospirillales	Alcanivoraceae	Alcanivorax	Alcanivorax_venustensis	OTU3383	0.0	0.0	0.0	0.0	1.8	0.0
Bacteria	norank	Proteobacteria	Gammaproteobacteria	Vibrionales	Vibrionaceae	Photobacterium	Photobacterium_profundum	OTU1176	0.0	0.0	0.0	0.0	0.0	2.4
Bacteria	norank	Proteobacteria	Alphaproteobacteria	Rhodobacterales	Rhodobacteraceae	Ruegeria	Ruegeria_mobilis	OTU1508	42.7	7.5	0.0	0.0	2.7	0.0
Bacteria	norank	Proteobacteria	Alphaproteobacteria	Rhodobacterales	Rhodobacteraceae	Labrenzia	Labrenzia_aggregata	OTU141	0.0	2.5	0.0	0.0	0.0	0.0
Bacteria	norank	Proteobacteria	Alphaproteobacteria	Rhodobacterales	Rhodobacteraceae	Labrenzia	Labrenzia_aggregata	OTU157	0.0	0.0	5.6	0.0	0.0	0.0
Bacteria	norank	Proteobacteria	Alphaproteobacteria	Rhodobacterales	Rhodobacteraceae	Labrenzia	Labrenzia_aggregata	OTU2164	0.0	0.0	0.0	22.1	0.0	0.0
Bacteria	norank	Proteobacteria	Alphaproteobacteria	Rhodobacterales	Rhodobacteraceae	Loktanella	unclassified_g__Loktanella	OTU1574	0.0	1.9	0.0	0.0	0.0	0.0
Bacteria	norank	Proteobacteria	Alphaproteobacteria	Rhodobacterales	Rhodobacteraceae	unclassified Rhodobacteraceae	unclassified_f__Rhodobacteraceae	OTU3432	0.0	16.2	0.0	0.0	0.0	0.0
Bacteria	norank	Proteobacteria	Alphaproteobacteria	Rhodobacterales	Rhodobacteraceae	unclassified Rhodobacteraceae	unclassified_f__Rhodobacteraceae	OTU1564	0.0	1.7	0.0	0.0	0.0	0.0
Bacteria	norank	Proteobacteria	Alphaproteobacteria	Rhodobacterales	Rhodobacteraceae	unclassified Rhodobacteraceae	unclassified_f__Rhodobacteraceae	OTU2109	0.0	0.0	0.0	1.3	0.0	0.0
Bacteria	norank	Proteobacteria	Alphaproteobacteria	Sphingomonadales	Erythrobacteraceae	Erythrobacter	Erythrobacter_citreus	OTU2102	0.0	2.9	0.0	2.3	0.0	0.0
Bacteria	norank	Proteobacteria	Alphaproteobacteria	Rhizobiales	Phyllobacteriaceae	Nitratireductor	uncultured_bacterium_g__Nitratireductor	OTU2146	0.0	0.0	0.0	3.3	0.0	0.0
Bacteria	norank	Bacteroidetes	Flavobacteriia	Flavobacteriales	Flavobacteriaceae	Zunongwangia	Zunongwangia_profunda_SM-A87	OTU2673	0.0	0.0	0.0	0.0	0.0	12.6